Ore Geology Reviews 137 (2021) 104279

Contents lists available at ScienceDirect

Ore Geology Reviews

journal homepage: www.elsevier.com/locate/oregeorev

IBERLID: A lead isotope database and tool for metal provenance and ore deposits research

S. García de Madinabeitia [a,*], J.I. Gil Ibarguchi [a,b], J.F. Santos Zalduegui [a]

[a] Department of Geology, University of the Basque Country (UPV/EHU), PO Box 644, E-48080 Bilbao, Spain
[b] Geochronology and Isotope Geochemistry Facility-SGIker, University of the Basque Country (UPV/EHU), PO Box 644, E-48080 Bilbao, Spain

ARTICLE INFO

Keywords:
Pb isotopes
Ore deposits
Iberian Peninsula
Balearic Islands
Database
Archaeometry

ABSTRACT

Although sometimes controversial, the use of Pb isotope data in geological research of ore deposits and metal provenance studies in archaeology has proved a useful tool for investigation of the relations between ore sources and raw materials used by humans. Users of this kind of information have often asked for complete datasets that would include not only numerical values of isotope ratios but also mineralogical and geological information about the samples analysed so as to allow for conscientious data comparison. The IBERLID database here presented has been designed to include available information for nearly 3000 samples from the Iberian Peninsula and Balearic Islands in a unique, complete to the extent possible, upgradable dataset using standardized variables. This allows to compare data and establish groups based upon isotopic ratios, mineralogy and other geological characteristics of the samples. The database is available through an online interactive public tool (www.ehu.eus/ibercron/iberlid) that provides for data search, comparison and graphics design, and may be furthermore exported for enhanced statistical treatment. By direct use of the proposed standardized variables, the compiled results allow to discern among 3 main mineralization events within the Iberian realm, while interpolation of Pb isotope data allow to draw the first maps of model age, mu and kappa parameters. The problem of radiogenic lead in some compiled data requires additional analyses of elemental concentrations, which so far has been generally neglected.

1. Introduction

Since the pioneering lead isotope analyses by Nier (1938), the application of lead isotope data in mineral exploration and assessment of age and source of ore deposits has been amply documented by many authors. Russell and Farquhar (1961) and Cannon and Pierce (1969), summarized and discussed available results for lead isotope data in relation to the problems of ore genesis and associated issues, and called for greater involvement of geologists in lead isotope investigations, until then greatly done by physicists and chemists. Continuing research on the subject involved progressively more Earth Sciences scholars and resulted in a wealth of studies, covered in due time by the synthesis book of Gulson (1986). Improvement in analytical techniques, in particular the introduction of multicollector plasma spectrometry (MC-ICP-MS) in the decade of 1990, gave rise to a dramatic increase of contributions and corroborated the relevance of lead isotope data as an essential tool in geochemical exploration methods (e.g., Bell and Franklin, 1993; Holk et al., 2003; Quirt and Benedicto, 2020). This also permitted the publication of a number of national-scale lead isotope maps for use in tectonic and metallogenic studies (e.g., Huston et al., 2019; Zhu, 1995).

The application of lead isotope data in provenance studies of archaeological metal artefacts may be dated back to the study of archaeological lead objects by Brill and Wampler (1967), which followed previous studies of Pb isotope composition in ore deposits like the aforementioned by Russell and Farquhar (1961) or Moorbath (1962) and other precursors. Pb isotope data have been regarded since then as a useful tool for the purpose because their different values: (i) are related to specific geological contexts, (ii) are not affected by weathering, and (iii) due to the limited range of atomic mass, they are essentially immune to modifications by metallurgical processes. During more than 50 years, many studies have thus been published that included Pb isotope ratios of ore deposits and of archaeological samples aiming to compare and assess the geological materials exploited in the antiquity for metal objects production. The way in which Pb isotope data have been employed in archaeological research has consisted in most cases in a straightforward comparison of a set of isotope ratios available from a database with

* Corresponding author.
E-mail address: sonia.gdm@ehu.eus (S. García de Madinabeitia).

https://doi.org/10.1016/j.oregeorev.2021.104279
Received 24 November 2020; Received in revised form 26 May 2021; Accepted 3 June 2021
Available online 6 June 2021

either those from a given artefact or collection of artefacts/ores, or, also, among individual artefacts/ores. The use of such databases of reference in archaeological studies of metal provenance is now widespread, different databases having been proposed since the 1990s, e.g., among others: (i) the Oxford Archaeological Lead Isotope Database (OXALID), which includes lead isotope data for ore deposits and archaeological artefacts, mostly from European sites, analysed at the Isotrace Laboratory of the University of Oxford in the years 1978–2001 (Stos-Gale and Gale, 2009); (ii) the Ore-Dataset v1 and v2 (Thompson and Skaggs, 2013) that includes Pb isotope data from ore deposits in the Peri-Mediterranean region; or, (iii) the compilation available from the Harvard Dataverse (Hsu et al., 2019) that incorporates currently available Pb isotope data for galenas and K-feldspars from China.

Although the usefulness of Pb isotope analyses in archaeological studies has been controversial (e.g., Pernicka, 1995; Pollard, 2009), its suitability in metal provenance studies is widely accepted nowadays provided a proper application that would take into account complementary archaeological and/or geological data (Artioli et al., 2020; Killick et al., 2020; Radivojević et al., 2019). In fact, the indiscriminate comparison of Pb isotope ratios from different sources and databases, sometimes without consideration of all possible sources and/or information on facts like data quality, sample origin and type of sample analysed can entail errors in source assignation (Radivojević et al., 2019). It is thus generally agreed that the interpretation of lead isotope values must be geologically sound and done in the context of all possible complementary material evidence to prevent untenable conclusions (Artioli et al., 2020). At the same time, improvements in analytical techniques have allowed to analyse not only Pb-rich minerals, but also whole rock and minerals with minor contents of Pb and sometimes significant amounts of U. This has resulted in a larger variety of lead isotopic data whose geological significance is now different since common Pb and radiogenic Pb may be included (Berger et al., 2019; Killick et al., 2020). Thus, and although the possibility of lead isotope analysis of a larger range of mineralizations represents an important advance in analytical achievements, it brings a necessary reflection on the way how all these data are to be used in the frame of geological and archaeological investigations.

Archaeology research groups working across Europe and the Mediterranean have researched in historical mining, metal metallurgy and commercial use of metals by the evaluation of lead isotope data lists for metal artefacts and exploited ore deposit. These data have been applied considering individual objects, hoards, regional assemblages and, even more broadly, the circulation of metals across time and space (Radivojević et al., 2019). By its geostrategic position and wealth of metal resources, the Iberian Peninsula has been a site of intense metal extraction through different historical periods (cf. Montero Ruiz, 2018).

The purpose of our study and of the proposed new database, IBERLID (Iberian Lead Isotope Database), is twofold. First, the compilation and assessment of the published Pb isotope data for minerals, rocks and archaeological objects from the Iberian Peninsula and Balearic Islands (Iberia or Iberian realm hereafter). This should allow for a better valuation of the data themselves and of the relation between geology, archaeology and lead isotope composition. On the other hand, the implementation of the new database for the Iberian realm is proposed as an exhaustive lead isotope compilation with geological perspective through the use of a public interactive tool: www.ehu.eus/ibercron/iberlid. In this way, analytical data for samples compiled in the database may be updated and processed in different manners by the users. This should provide an advanced alternative tool for studies of metal provenance incorporating at the same time geological and mineralogical information.

In IBERLID we have collected Pb isotope data from a great number of studies that have been published in a variety of monographs, reports and journals, the latter mainly mineralogical or archaeological, with manifest different criteria of publication. As it happens, the dispersion in the type of presentation and the scarcity of multidisciplinary research teams often hinders the proper exploitation of the analytical results. The use of a new database with standardized variables and geological perspective is thus proposed as a solution to this problem pointed out in recent publications (Montero Ruiz, 2018; Schibille et al., 2020). Furthermore, the present compilation should help in interpreting measured Pb isotopic compositions in terms of geological evolution of different areas within the Iberian Peninsula.

2. Geological and metallogenic characteristics of the Iberian Peninsula and related areas

The complex geology of the Iberian Peninsula includes from rocks generated in superficial sedimentary conditions to continental and oceanic remnants obducted from subduction zones, together with a great amount and variety of igneous intrusives, mostly granites s.l., fragments of lithospheric upper mantle and various types of young Neogene to Quaternary volcanic areas. Exposed rocks broadly cover the last 600 Ma of Earth's history. This complexity is also reflected in the ample typology of ore mineral deposits. Types and volume of mineral deposits are widely variable. There are magmatic- (plutonic, volcanic and hydrothermal), shear-zone-, sedimentary- and stratabound-related ore deposits that range from scattered and artisan exploitations to giant ore deposits. Also, different metallic ores have been exploited during the long history of mining activity since, at least, the 3rd Millennium BC (Lunar et al., 2002). These have been classical ore sources for metal objects found in many archaeological sites both within and outside Iberia (cf. Jézégou et al., 2011; Wagner, 2000; Westner et al., 2020; Wood and Montero-Ruiz, 2019; etc).

Attending to the principal tectonic events recorded, the geology of Iberia can be categorized into 3 main domains (Fig. 1): (1) the Variscan and pre-Variscan areas, best represented within the so-called Iberian Massif, a part of the European Hercynian foldbelt, where rock units mainly result of the Variscan and Cadomian orogenies; (2) the Alpine areas, which refers to sections affected by the Afro-Iberian-European plate collision as part of the large Alpine-Himalayan collisional belt; and (3) undeformed or nearly undeformed sedimentary areas of Cenozoic to Quaternary age that developed in relation to the great rivers of the Peninsula and partially overlie the two older areas (Fig. 1). Neogene to Quaternary volcanic areas do not form a single region but account for a great number of scattered exposures around the Cabo de Gata, Calatrava and Olot regions. For extended accounts on the geology of Iberia we refer the reader to the synthesis volumes by Gibbons et al. (2002), Vera (2004) and the book series by Quesada et al. (2019). In the following, a brief summary is presented for the purpose of the present study.

The so-called Iberian Massif is the largest expanse of Pre-Permian rocks within the Iberian Peninsula and has been classically divided into 5 main tectonic zones (Dallmeyer et al., 1990; Julivert et al., 1972). Taking into account their main geological features, we have adopted a simplified classification into just 3 areas with distinctive features (Fig. 1): the northern branch of the Iberian Massif (NIM), the Ossa-Morena Zone (OMZ) and the South Portuguese Zone (SPZ). The NIM comprises 3 of the 5 classical tectonic zones of the Massif sharing a number of tectonostratigraphic features (Julivert et al., 1972): the Cantabrian Zone, the West Asturian-Leonese Zone and the Central Iberian Zone. Variably metamorphosed subautochthonous Precambrian to Permian marine sedimentary rocks, and allochthonous high-pressure metamorphic units, together with abundant igneous intrusives form this northern branch, all of them attesting to Variscan s.l. tectonothermal events. Towards the south of it, the Ossa-Morena Zone (Fig. 1) has been considered as a separated area because of the abundance of rock units formed on the margin of Gondwana during the late Neoproterozoic-Lower Paleozoic Cadomian orogeny. These were intensely reworked subsequently during the Variscan orogeny and arranged in bands with NW-SE trends. The southernmost area of the Iberian Massif, the South Portuguese zone (Fig. 1), is regarded as a piece of

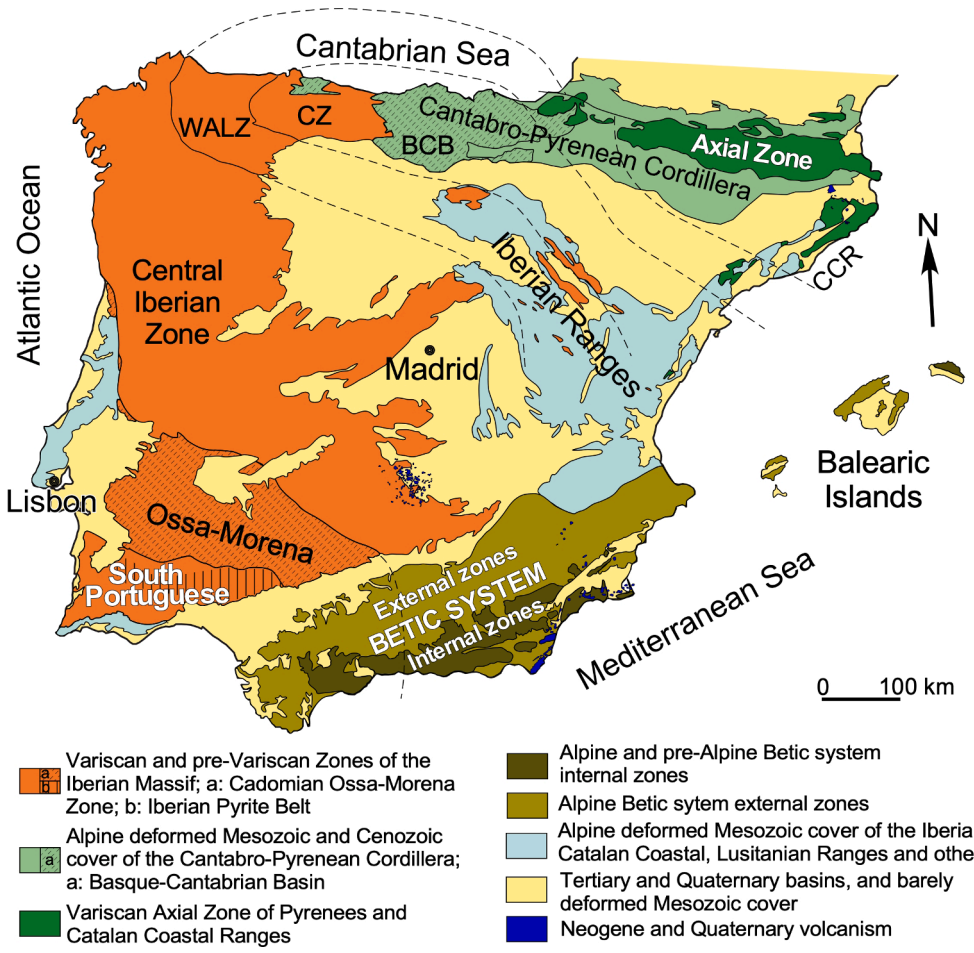

Fig. 1. Iberian Peninsula and Balearic Islands simplified geological map with geological zones included. Modified from Julivert et al. (1972) and Muñoz (2019).

a different continent separated from the OMZ by a band of metamorphosed mafic rocks known as the Beja-Acebuches ophiolitic complex (Simancas et al., 2004 and refs. included). The SPZ consists essentially of marine sediments formed since Devonian to Permian with numerous intercalations of volcanic rocks. It is in this Zone where is located a very distinctive mineral deposit: the Iberian Pyrite Belt (IPB) made of supergiant massive sulphide deposits including among the world's largest mines (Rio Tinto and others).

Rock units essentially affected by the Alpine orogeny are much less abundant and appear in two different areas: (i) the Betic System or Betic Cordilleras (BC) in the southeast and their extension into the Balearic Islands in the Mediterranean Sea, and (ii) the Cantabro-Pyrenean Cordillera in the north and northeast including the so-called Basque-Cantabrian Basin and the Catalonian Coastal Ranges on its west and east sectors, respectively (Fig. 1). Both the Betics and the Cantabro-Pyrenean realms comprise Mesozoic to Cenozoic materials, some Precambrian and Paleozoic cores (e.g., Pyrenees Axial Zone, Betic Internal Zones) and conspicuous ultramafic rocks (e.g., the 300 km^2 Ronda peridotite massif or the type locality of lherzolites at Lherz, among others). These two main areas are considered the westernmost extent of the Alpine-Carpathian-Himalayan orogenic system. Pre-Mesozoic basement cores there were affected by the Variscan and possibly the Cadomian orogeny, while surrounding Mesozoic or Cenozoic units were deformed by the Alpine orogeny. A distinctive unit among the Alpine terranes is the Basque-Cantabrian Basin (BCB) located between the Pyrenees s.s. and the Cantabrian Zone of the northern branch of the Iberian Massif (NIM). Pre-Mesozoic units in this sector are absent, while there exists a thick pile of sediments (>10 km) including siliciclastic and evaporitic deposits, reef-limestones and volcanic and pyroclastic rocks deposited since Mesozoic to Cenozoic. As it will be shown below, this sector of the Pyrenean realm presents distinctive Pb isotope characteristics that justify its consideration as a separate entity of the Alpine system.

Besides the above mentioned areas that record deformation, metamorphic and magmatic events related to the Cadomian, Variscan and Alpine orogenies, near a half of the surface of the Iberian Peninsula is covered by Cenozoic to Quaternary deposits related to the great river basins of the Ebro, Douro, Tagus and Guadalquivir rivers. In these areas there are no important ore deposits, just some isolated ones related to underlying materials.

Neogene to Quaternary volcanic areas are found in the southeast, south-central and northeast Iberia. Neogene volcanism of the southeast is related to the Alpine cycle and forms extensive outcrops of calc-alkaline rocks around Cabo de Gata. It is associated to the formation of important mineralizations (e.g., Rodalquilar), while high-K and shoshonitic rocks, lamproites and alkali basalts form smaller outcrops along more than 200 km towards the NE of the area. Numerous outcrops of volcanic rocks in the Calatrava volcanic field (south-central Iberia), onshore and offshore of Valencia and in the sector of Olot and nearby areas (northeast Iberia) are of a different style. They are made of alkaline rocks related to the rift system in Central and Western Europe that evolved in the Alpine foreland during late Eocene to recent times and do not associate significant ore deposits.

3. The database

The use of lead isotope analyses in geology and archaeology is based on the physical and chemical properties of this element. There are four isotopes of Pb, three of them are radiogenic products of radioactive

decay: ^{208}Pb is produced by the decay of ^{232}Th, ^{207}Pb by that of ^{235}U, and ^{206}Pb by that of ^{238}U. The isotope ^{204}Pb is not the product of any radioactive decay for which reason its amount does not change during the geological history. Because radioactive decay is irreversible, the Pb isotope ratio in every system containing U and Th will change with time. Thus, the $^{206}Pb/^{204}Pb$, $^{207}Pb/^{204}Pb$ and $^{208}Pb/^{204}Pb$ ratios will increase consistently with time. This important characteristic of the Pb isotopic system is a useful asset in geological sciences and has been extensively used for studies of age and geological evolution by means of isotope analyses of rocks and minerals. When an ore mineral, rock or system is formed, its U/Pb ratio is established and it is therefore specific for each particular case. Some minerals may incorporate U and/or Th relatively easily in their structure but not Pb, zircon is a typical example. Other minerals barely incorporate U and/or Th but contain significant amounts of Pb, the usual process in galena and other Pb ores. The different evolution of Pb isotopic ratios in each case is clear: the Pb isotopic ratios of a zircon will be due to the radioactive disintegration of U during the time elapsed since the formation of the mineral; instead, the lead isotopic composition of the galena will keep unchanged through time. The Pb isotopic ratio of a given sample will be therefore different from another one depending on the amount of Pb, U and Th incorporated in its structure. These variations in U/Pb and Th/Pb in different sample types are the ground for the use of the uranium-lead isotopic system in geological and archaeological studies. While some minerals like zircons are thus very appropriate to establish the age of geological events, others, like galena, are good indicators of the properties of the system during mineral formation (Allègre, 2008; Dickin, 2018).

In sulphide ores, like those exploited as ore deposits since ancient times, U was generally not incorporated into the mineral structure. In this way, the Pb isotopic composition was frozen at the time of the ore-forming event ensuring that it would retain a constant Pb isotopic composition and provide an individual Pb isotope fingerprint. Besides that, the isotopic composition of a heavy element like lead does not change by natural processes or during the handling of Pb-bearing ores or metals. Whether they are affected by roasting or smelting, cupellation, melting, alloying, dissolution or corrosion, the isotopic composition of the lead component remains constant. Therefore, the isotopic composition of the Pb-bearing ore mineral and the archaeological metal artefact manufactured from it will show the same Pb isotopic ratio. This will be a constant ratio related to the geological properties of the lead source. The isotopic composition of this Pb in minerals devoid of U and or Th is the so-called common Pb. It is employed to calculate model ages and other parameters whose value depends on an assumed model and hence not accurate enough for dating purposes in geology. However, the common Pb composition and the calculated model age are good indicators about the type of geological ore forming event and may constitute an efficient way to discriminate metal sources (Desaulty et al., 2011). Despite this ability of model ages and other isotopic parameters like μ ($^{238}U/^{204}Pb$) and κ ($^{232}Th/^{238}U$), which are common tools as ore provinces discriminators in geological studies, they have been rarely used in archaeometry. In this respect, and while some authors see the use of graphs employing these parameters in archaeometric studies as sources of inaccuracy (Villa, 2016), their implementation and utility are becoming increasingly significant (Albarède et al., 2012; Killick et al., 2020).

Whatever the case, the use of just lead isotope ratios implies a basic assumption not always fulfilled, which is that every analysed sample must carry very low or negligible amounts of U and Th contents to guarantee that U/Pb and Th/Pb ratios are near to zero. In cases where U and Th contents in a given sample are not that insignificant, the measured ratios will be the result of a combination of common Pb composition inherited from the source, and the Pb generated by radioactive disintegration of U and Th since the formation of the mineral. In such a case, the lead isotopic ratios in a given ore deposit will not keep constant for different minerals and, while galenas and other Pb minerals will show the same ratios, other minerals with higher U/Pb or Th/Pb values will carry more radiogenic Pb and thus, present higher values in those ratios including ^{204}Pb as denominator.

These physicochemical properties of Pb isotopes have extended the use of this tool in geological research of ore deposit genesis and in archaeological studies of metal provenance. Yet, the extensive use of lead isotope analysis (LIA), with thousands of analyses of great variety of samples and hundreds of provenance studies based on those data, has also revealed the problems derived of the use of Pb isotopic data done only on account of numerical comparisons as is often the case. A correct use of Pb isotopic ratios would require of complete isotopic databases with geological and mineralogical information (Artioli et al., 2020, 2016). This would allow to solve the biggest pitfall detected in provenance studies: incomplete database support and partial or biased contextual information, which are among the facts at the origin of fierce discussions on the validity of LIA in archaeology during the last decades (e.g., Artioli et al., 2020; Gale, 2009; Pernicka, 1995; Pollard, 2018, 2009). In addition, the lack of standardized rules for the publication of data (Artioli et al., 2020) and the use of the techniques like magic bullets, without proper consideration of the limitations imposed by the geology (Killick et al., 2020), makes difficult to compare with one another the large amount of published data.

In this work we present a new public database, IBERLID, standardized, rationalized, accessible and complete to the extent possible. The IBERLID database is intended to allow for a less problematic use of lead isotope results and make easier their comparison. The compilation and evaluation of data from nearly three thousand lead isotope analyses is expected to contribute and expand the knowledge on the geology and isotopic composition of ore deposits of the Iberian Peninsula and Balearic Islands. At the same time, this should allow for an improved use and a better interpretation of Pb isotopic data in studies of metal provenance in archaeology. The IBERLID database is not just an extensive table of lead isotope ratios. As described in the following paragraphs, it also includes interactive tools linking isotopic ratios, geographical, geological, mineralogical and archaeological information, thus providing new ways for sample data selection, pooling and comparison.

3.1. IBERLID

The IBERLID database has been designed to make the comparison and appraisal of available Pb isotopic data for samples of the Iberian Peninsula and Balearic Islands easier and in a more conscious way by including complementary information of various types. The criteria used to create the database are listed herein: (i) the database incorporates all the essential data reported in the original publications, specially those on the type of samples analysed and additional sample information; (ii) it allows for a statistical treatment of the data and their intercomparison; (iii) all the data, and specially those related to ore deposits are geolocalised using conventional coordinates; (iv) it includes the possibility of updating and increase the number of samples compiled; and (v) it is an open access database. Based on these criteria, we have developed the database as an open data source and made it accessible to the users in two ways: (1) through an interactive public web site (www.ehu.eus/ibercron/iberlid), where all the data are represented or may be represented by the user in a number of exportable selected diagrams, maps and tables, and (2) through a detailed spread sheet (cf. Supplementary material) that includes all the compiled data and allows further handling by the users through specific statistical software of their choice. The web site holding the database and also all the graphs, tables, sample groups and calculations have been implemented using RStudio, an integrated development environment for R in open source edition that runs on the desktop in Windows, Mac or Linux operating systems. The corresponding scripts for data pooling, graphs and calculations are included in Supplementary material.

The interactive public web site (www.ehu.eus/ibercron/iberlid) includes, in different tabs, directly compiled data for geological and

archaeological samples and a tab for filtered data, where the criteria used in this work for data filtering and grouping are applied. The interactivity allows sample selection based on different filters, including a map for direct choice of area, selection of type of sample analysed, as well as other specific criteria assigned to each tab, like geological zone or manufacturing period. After a selection of the samples of interest, some graphs are automatically obtained including, among others, graphs of Pb isotopic ratios grouped by geological zones, box plots of isotopic ratios classified by the reference where the data where published and 3D graphs, where $^{206}Pb/^{204}Pb$, $^{207}Pb/^{204}Pb$ and $^{208}Pb/^{204}Pb$ ratios are used as graph axis. All of these plots are interactive; allow to adjust some image parameters, as axis dimensions; show pop-up messages with data information and it is possible to exclude represented samples. Besides the diagrams, selected data can be obtained in a detailed table, where analyses can be sorted, checked and exported.

3.2. The variables of the database

The IBERLID database constitutes a compilation of lead isotope analyses of geological and archaeological samples obtained from different sources. To increase the usefulness of this compilation, the database includes all available information considered of interest in the original papers. Hence, different variables have been taken into account going from sample type, geographic names and so on, to published isotopic ratios and element concentrations when available, and also new variables computed for the purpose from the published data (see below). Table 1 shows all the variables considered in the database. Some details on the main variables are given in the following lines.

All the samples are geolocalised by means of WGS 84 Web Mercator coordinates to facilitate the integration of studies carried out by researchers of different scientific disciplines, in particular geology and archaeology. Such information was obtained either from the published geographical sample data or, in most cases, has been established by using the more or less precise information provided in the original publications and geographical maps available online from national and regional institutions. All latitude and longitude data are in decimal format and have been used to obtain sample map locations (Fig. 2). The accuracy of the coordinates provided reflects obviously the quality of the geospatial information available in the publications for each ore/sample. This implies that the specific location listed in the database could be in cases up to a few 10–100 s meters of the actual mining site or collection point mentioned in any given publication. Some archaeological samples, usually coins or ingots, although have been related by the authors to specific Iberian ore deposits, have no information about the precise sampling location (i.e. Albarède et al., 2016; Birch et al., 2020; Brill et al., 1987; Sinner et al., 2020; Stannard et al., 2019). Those samples have been placed in fictitious locations of the Mediterranean Sea (Fig. 2).

Information for each sample is provided through a number of variables included in the database. For a start, two main standardized categories of samples may be considered: (1) geological samples, which are those samples with a direct relationship between isotopic data and sample location, and (2) archaeological samples, when the relation between sample and geological/geographical information is not immediate due to the possibility of some type of material transport or treatment. However, to enable a first handling of the compiled data through the selection of specific types of samples, this may be done more precisely and to this purpose we have included a variable called *sample.type*. The values proposed for this variable allow for a rapid classification and differentiate between: (i) *mineral samples*, which are those minerals collected directly at the ore deposit or related materials; (ii) *rock samples*, these are typical geological samples that involve whole rock dissolution and analysis; (iii) *archaeological artefacts*, here defined as any metallic object produced or given shape by humans, be it a tool, a weapon, a work of art, etc., implying transformation of metals or minerals by metallurgical processes; and (iv) *archaeological site MBP* (abbreviated for archaeological site minerals and by-products), this variable includes: (a) natural ore minerals found in archaeological sites, that is, minerals that are not in situ but are assumed to have been transported from the original ore deposit, thus bearing no relation to the geology of the sampling site; (b) waste minerals (like jarosite) or secondary minerals (litharge) produced in relation to the site metallurgical, stocking, etc. activity, and (c) by-products of this activity like slags or clinkers. Although the two types of archaeological samples are sometimes found close to mineralizations, we have considered for simplicity that they do not provide direct information about their geological source due to the eventual transportation from the mine to the archaeological site.

Detail maps for sample situation are provided in the database site www.ehu.eus/ibercron/iberlid and may be handled at different scales through the zoom tool. The location of any sample is basic information to place it in a geological context. For the geological samples group the sample location is directly related to the geological zones established in the introduction, namely in alphabetic order: (i) Betic Cordilleras (BC), including samples from the Balearic Islands, (ii) Basque-Cantabrian Basin (BCB), (iii) Catalonian Coastal Ranges (CCR), (iv) Northern branch of the Iberian Massif (NIM), (v) Ossa-Morena Zone (OMZ), (vi) Pyrenees (Py) and (vii) South Portuguese Zone (SPZ) (Fig. 2). A first geological information is thus introduced in the database under a new variable called *geological.zone*. This standardization improves the sample grouping and may be further used for data description and discussion. Also, additional information when available for this group is included in the database under the following five variables: *sample.details*, *geol.age*, *host.rock*, *deposit.morphology* and *realm* (Table 1).

In the case of the group of archaeological samples, their location is circumstantial information, whereby a variable of the type *geological.zone* proposed for the geological samples is impossible. In this case the variable selected, based on the narrative of the artefact according to the original study, is *period*. This is an intrinsic characteristic of the sample that allows establishing different data groups. We have defined 8 standardized values within the *period* variable (see Table 1C), including one called *unknown* for those cases where the pertinent information is not provided in the original publication. Additional information in each case is specified under a variable termed *chronology* following the format used in the corresponding source.

Standardized lead isotope sample information allows to classify and compare the compiled data of selected samples. Isotopic ratios standardization requires the use of the same parameters, not only in ratios but also in errors. Thus, the information for the values of five Pb isotopic ratios is provided: $^{206}Pb/^{204}Pb$, $^{207}Pb/^{204}Pb$, $^{208}Pb/^{204}Pb$, $^{207}Pb/^{206}Pb$ and $^{208}Pb/^{206}Pb$, either taken from the original publications or computed from the published data when they were not provided. The analytical error or uncertainty of the isotope ratios is reported when this was stated in the original publication and always listed as 2σ in absolute values. Besides the isotopic ratios, additional variables have been added in the database. These variables are parameters rarely given in publications dealing with lead isotope data in archaeology, although are common in geological publications; in those cases, the original values are compiled in the database as *model.age*, *mu* and *kappa*. However, and in view of their potential interest for studies of metal provenance, we have calculated or recalculated these parameters for all the samples and added them to the variables of the database. These variables are named as follows: *tmod* (model age) in Ma, *mu12* (μ) = $^{238}U/^{204}Pb$ and *kappa12* (κ) = $^{232}Th/^{238}U$. All of them have been computed using the MATLAB solver of Albarède et al. (2012), updating the $^{238}U/^{235}U$ value to 137.79 (Andersen et al., 2017) and using the Stacey & Kramers model (Stacey and Kramers, 1975).

Table 1
Variables included in the database and standardized values used in variables (more detailed description included in text).

VARIABLES	
NAME	**EXPLANATION**
code	New code for each analysis. Unique.
sample	Sample number used in original work
country	Country were the sampling point is located.
province	Province or area were the sampling point is located. Based in assigned geographical coordinates
location	Town were the sampling point is located. Based in assigned geographical coordinates
outcrop	Mine or archaeological site name used in original work.
decimallatitude	Cartesian coordinate System based on WGS 84 (EPSG:4326)
decimallongitude	Cartesian coordinate System based on WGS 84 (EPSG:4326)
sample.type	New parameter. Can be: WR, Mineral, Archaeological artefact or Archaeological site MBP.
analysed.material	Simplified variable for chemical composition of analysed sample (see text and Table 1A).
sample.details	Detailed information about the sample, like specific minerals or type of archaeological artefact analysed.
main.ore	Simplified version of type of mineralization samples including only 2 elements in alphabetic order. Information from original paper or from mining district (when the first option is not available).
p206.204	$^{206}Pb/^{204}Pb$ compiled from original paper. When this ratio was not published, calculated from other ratios.
p206.204.2sd	Analytical errors in the original paper, recalculated to 2σ in absolute value when needed.
p207.204	$^{207}Pb/^{204}Pb$ compiled from original paper. When this ratio was not published, calculated from other ratios.
p207.204.2sd	Analytical errors in the original paper, recalculated to 2σ in absolute value when needed.
p208.204	$^{208}Pb/^{204}Pb$ compiled from original paper. When this ratio was not published, calculated from other ratios.
p208.204.2sd	Analytical errors in the original paper, recalculated to 2σ in absolute value when needed.
p207.206	$^{207}Pb/^{206}Pb$ compiled from original paper. When this ratio was not published, calculated from other ratios.
p207.206.2sd	Analytical errors in the original paper, recalculated to 2σ in absolute value when needed.
p208.206	$^{208}Pb/^{206}Pb$ compiled from original paper. When this ratio was not published, calculated from other ratios.
p208.206.2sd	Analytical errors in the original paper, recalculated to 2σ in absolute value when needed.
pb.content	Information from the original paper when it is provided.
u.content	Information from the original paper when it is provided.
model.age	Information from the original paper when it is provided.
mu	Information from the original paper when it is provided.
w	Information from the original paper when it is provided.
geological.zone	Only available for geological samples. Based on mayor geological divisions of the Iberian Peninsula and information provided in the original paper (see text and Table 1A)
geol.age	Information from the original paper when it is provided.
host.rock	Type of rock were the ore deposits appear. From original paper.
deposit.morphology	Information from the original paper about mineralization.
realm	Information from the original paper about mineralization.
excavation.no	Information from the original paper about archaeological site and sampling point.
find.spot	Information from the original paper about archaeological site and sampling point.
courtesy	Information from the original paper about archaeological site and sampling point.
period	Information simplified from the original paper (see text and Table 1C).
chronology	Information from the original paper about specific sample datation.
tmod	Model age in Ma, calculated by Albarède et al., 2012
mu12	μ (238U/204Pb), calculated by Albarède et al., 2012
kappa12	κ (232Th/238U), calculated by Albarède et al., 2012
reference	Original paper in which data appears
ref.code	Unique code for each source, only to simplify grouping and graphs.
laboratory	Laboratory where analyses were done.
spectrometry	Spectrometric method employed (MC-ICPMS; TIMS; Q-ICP-MS)
observations	Notes about the sample or the analysis

TABLE 1A: analysed.material	
VALUE	**INCLUDE…**
Cu metal	Includes those samples with high contents in Cu, also different types of bronzes
Fe mineral	Pyrite, Pyrrhotite, Arsenopyrite, Hematite, Goethite, Magnetite, Jarosite
Galena	Analysis of handpicked galena.
Gold	
Hg mineral	Cinnabar
Litharge	
Ore mix	Used for whole rock mineralized and in those cases when minerals are not separated for analysis. Details in sample.details.
Other	Calcite, Fluorite
Pb metal	Used in those cases of archaeological materials, with different uses but mainly composed by Pb
Pb mineral	Includes not identified sulphides, sulfosalts, cerusite
Sb mineral	Stibnite
Silicate	K-Feldspar, Diopside, Vesuvianite
Silver	
Slag	Material with undetermined characteristics.
unk	when the analysed mineral is not identified
Whole rock	Used for rocks not mineralized. Description in sample.details
W mineral	Wolframite
Zn mineral	Sphalerite

TABLE 1B: geological zone	
CODE	**DESCRIPTION**
BC	Betic Cordilleras
BCB	Basque-Cantabrian Basin
CCR	Catalonian Coastal Ranges
CIZ	Central Iberian Zone
NIM	Northern branch of the Iberian Massif = West Asturian Leonese Zone + Central Iberian Zone + Cantabrian Zone
OMZ	Ossa-Morena Zone
Py	Pyrenees
SPZ	South Portuguese Zone

TABLE 1C: period	
VALUE	**INCLUDE…**
Bronze Age	Late Bronze age, Phoenician, Tartessian, Argaric
Copper Age	Chalcolithic
Greek	
Iron Age	Ibero-Punic and Iberian
Roman	Roman Republican and Roman Imperial
S. X	
s. XV	
Stone Age	Neolithic

3.3. Summary of data, tables and graphics generated by the tool

As previously stated, all the data in IBERLID may be handled by the user and either exported directly in the form of selected diagrams, maps and tables, or downloaded for further handling through specific software. In the following, we summarize the information provided in the database and show typical examples of the graphs and other details.

The current compilation includes 2977 analyses performed in 45 different laboratories and published in 140 studies. 1467 determinations were done by Thermal Ionization Mass Spectrometry (TIMS) methods, 1413 by Multi Collection Inductively Coupled Mass Spectrometry (MC-ICP-MS) methods and 97 by Quadrupole Inductively Coupled Mass Spectrometry (Q-ICP-MS). Most analyses listed in the database (997 samples) have been performed at the SGIker facility of the University of the Basque Country (Spain) for different archaeological and geological research groups. Other laboratories that have greatly contributed to the compilation were the Isotrace Laboratory at the University of Oxford (353 samples), the Goethe University from Frankfurt (276 samples) and the French Geological Survey (BRGM, 173 samples). The rest of the laboratories, up to 45 from different institutions, have contributed with 1178 data (Table A1).

The distribution of data among the four sample types defined above is as follows (Fig. 3A, Table A2): (i) mineral samples, 50.62%; (ii) rock samples (WR), 2.18%; (iii) archaeological artefacts, 43.47%; (iv) archaeological-site MBP, 3.73%. Thus, the two large groups of samples in the database are geological samples with 52.80% of the total and archaeological ones with 47.20% of the data (Fig. 3B, Table A3).

The geological information available for the mineral samples and rock samples groups is heterogeneous and highly depending on the aim of the original work. Some data are collected from geological studies with detailed information about ore deposit characteristics, while others were obtained from publications with a historical vision of the mining activities and almost devoid of just containing basic geological information. As a consequence, the use of detailed geological information for statistical purposes has been discarded. However, all the data include, at least, a useful variable in this regard (*geological.zone*) that allows to group the samples according to their geological location (Fig. 2). Out of the 787 values of sample types recorded under the variable *sample.details,* a standardized *analysed.material* variable allows for a significant reduction to 22 main values. According to the *analysed.material* variable, most data correspond to analyses of galena (42.68% of the samples) with also an important proportion of Cu minerals (23.73%) and of what we have termed ore mix (13.04%) for those cases when the analysed sample includes more than one type of ore mineral (Fig. 3B, Table A4).

In the archaeological samples group, samples are mainly alloys and sometimes pure metals. These samples have been classified by the most abundant element, resulting the next groups and abundances: the so-called Cu metal (37.37%) group formed by materials with high Cu contents; Pb metal (25.62%), where Pb rich samples are included; and silver (16.37%) for those samples where Ag is the main constituent; while other materials like slag (7.83%), galena (3.56%), Sn metallic samples (2.14%) or gold (1.49%), among others (Fig. 3B, Table A5), account for less than 10% each of this group.

Although the isotopic information for the archaeological samples is not necessary related with the sampling site due to the eventual transport of raw materials, a crude vision of the spatial relation between ore mineral sites and archaeological sites may be observed (Fig. 2). Since the geological characteristics of each region can be continued across geography, similar possible relations between ore deposits and archaeological sites could be expected or searched for. As previously mentioned, the variable *geological.zone* was not given any value in the archaeological samples group. However, in this case the additional variable *period*, based on the archaeological age established for each site, has been established for data pooling. Thus, according to the simplified scheme shown in Table 1C, 52.41% of the samples are from the Bronze Age, 36.64% correspond to Roman era samples and the rest of periods show frequencies much lower, like 6.93% of samples from Copper Age or 3.46% of samples are from the Iron Age. There are 77 samples compiled in the database, that is, 5.48% of the total (Table A5), that do not carry information about the archaeological period.

The limited information about analytical methods provided in many publications is revealed by the fact that error data are available for less than 42% of the samples included in the database. Both the analytical errors and the decimal figures in the isotopic ratios listed have been a matter of concern during the compilation of data. This is a consequence of the great dispersion in the editorial rules for data display. As a result, the compulsory relation from an analytical point of view between decimal positions and analytical errors is not always fulfilled. To avoid any bias, the significant figures used in the compilation have been the same used in the source of each data.

The isotopic ratios for all the samples compiled in the database and the frequency of each ratio are shown in the Fig. 4 and Table A7. The whole set of data shows a great dispersion of values ranging from 17.44 to 87.76 in $^{206}Pb/^{204}Pb$, from 14.98 to 19.74 in $^{207}Pb/^{204}Pb$ and between 36.74 and 49.43 in $^{208}Pb/^{204}Pb$ ratio. The different dispersion of the ratios is evident in the diagrams on the marginal graph where also the archaeological and the geological samples show a frequency peak around the mean ratios of 18.77 for $^{206}Pb/^{204}Pb$, 15.68 for $^{207}Pb/^{204}Pb$ (Fig. 4) and a less representative peak around 38.59 with higher dispersion of the values for the isotopic ratio $^{208}Pb/^{204}Pb$ (Fig. 4). The results obtained for the seven groups of geological samples and the group of archaeological samples are commented more in detail below.

The distribution of geological samples in different geological zones reflects the historic importance of mining in different areas. Thus, near 34.03% of the samples are located in the northern branch of the Iberian Massif, 20.61% of the samples are from the Betic Cordilleras, 17.75% of the data corresponds to the South Portuguese Zone and 13.17% are from the Ossa-Morena Zone. The other 3 areas, Basque Cantabrian Basin, Catalonian Coastal Ranges and Pyrenees are much less represented (Fig. 2 and Table 2). The statistics for isotopic ratios and related parameters for each geological zone is summarized in the Table 2 and Fig. 5, where all the parameters have been calculated for 2 different groups of samples: (1) on one hand, all the geological samples classified by their corresponding geological zone (Fig. 5A), and (2) only the samples of galena, also grouped by geological zone (Fig. 5B). If we take into account the whole set of geological samples (Table 2A and Fig. 5A), it may be observed that while some of the geological zones, like BC or BCB, show fairly homogeneous isotopic ratios with deviations of values <0.3 for all the isotopic ratios considered, in other zones the isotopic ratios are much more variable, like the extreme case of the NIM making the graphs obtained (Fig. 5A) totally conditioned by such a large dispersion. Geological zones defined by Julivert et al. (1972) are based on the main tectonic characteristics of each area although this does not mean that within each geological zone all the materials are homogeneous. Although source of the dispersion in isotopic ratios could thus be related to geological heterogeneities within each geological zone, there is an evident relation with the type of mineral analysed. This that can be easily observed by comparing the isotopic ratios of the whole set of geological samples (Table 2A and Fig. 5A) with the values for the galenas (Table 2B and Fig. 5B): the dispersion in the isotopic ratios decreases drastically, e.g., in the NIM the SD value for $^{206}Pb/^{204}Pb$ ratio changes from 6.04 to 0.21 (Table 2B and Fig. 5B).

In the case of the archaeological samples (Table 3) the dispersion is considerably smaller than in the geological samples, with a maximum SD of 1.26 in the $^{206}Pb/^{204}Pb$ ratio. Though geographical or geological groups are not considered in the case of archaeological samples, the

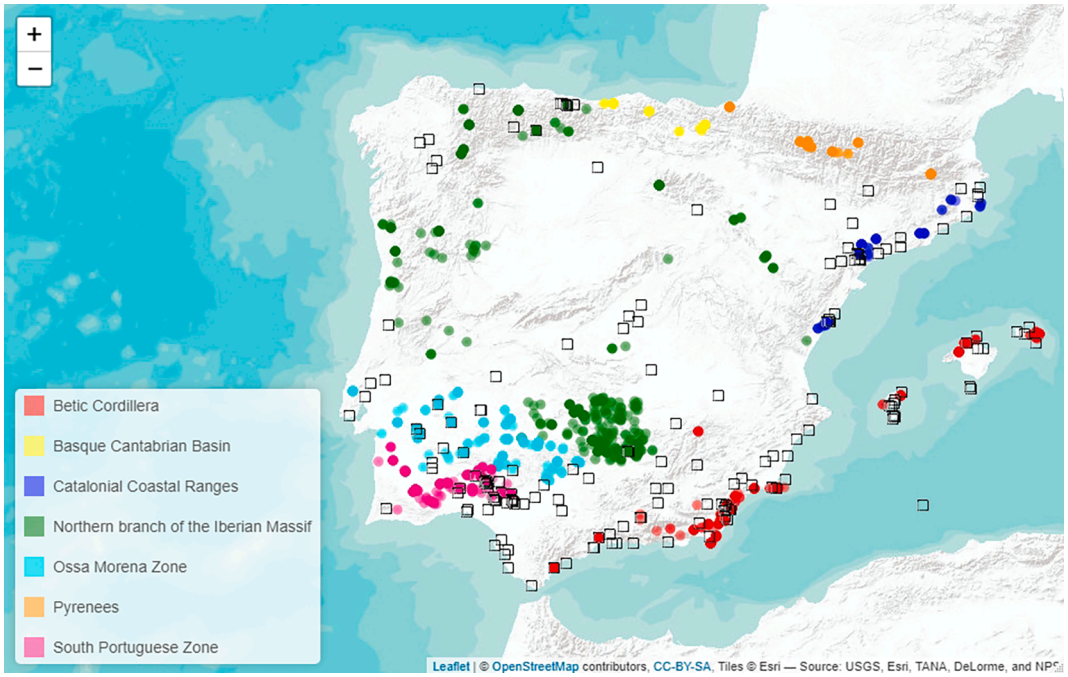

Fig. 2. Distribution map of all of the samples in IBERLID. Open squares are archaeological samples; geological samples are represented by coloured circles. The colour legend included in this graph is also employed in other graphs in this work.

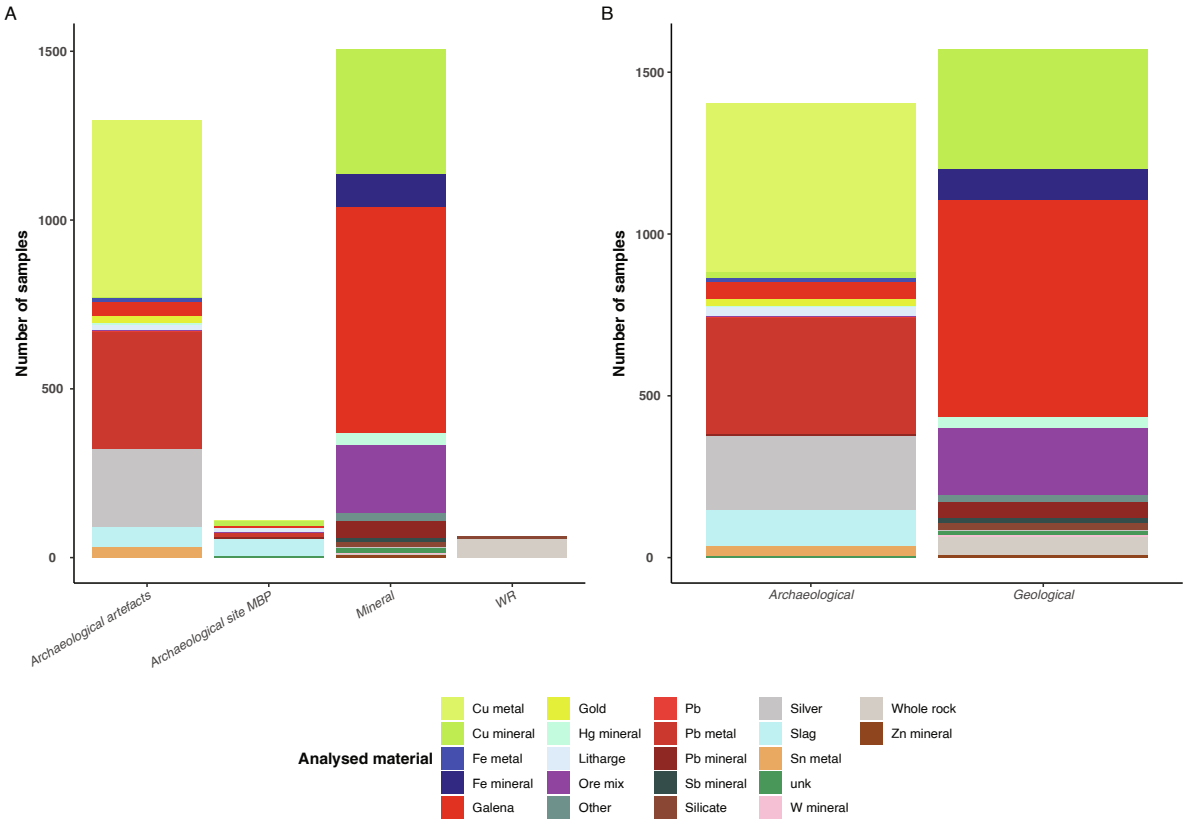

Fig. 3. Graphical frequency of variables that include mineralogical information for IBERLID samples. A) Number of samples included in each value of *sample.type* variable; B) number of samples included in each sample type after simplification. Each colour used in bars indicates different type of material analysed. Data points plotted as 'unk' correspond to analyses from samples lacking proper identification in the data source. For instance, leachates in Higueras et al. (2005) or samples without description in Rodríguez Vinceiro et al. (2018). The same colour legend is used in other figures in this work.

relation between dispersion of isotopic ratios and type of analysed material is also evident and, while Pb metals and silver samples show reduced dispersions, Cu metals data drastically increase the dispersion (Fig. 6 and Table 3).

Although model age, μ and κ parameters are calculated for all the samples, the computation is strictly valid only for those samples with μ ≈ 0, that is, samples that have very low U contents (Albarède et al., 2012). Model ages obtained range from −223237 to 1095 Ma, μ values from 0 to 86.54 and κ values from 0 to 5.25 (Fig. 7, Table A6). The complete set of results shows that an important number of samples would have future ages (negative values), reflecting the problem of model age calculations in ore samples when radiogenic lead has been analysed. However, when only Pb samples are considered the negative values are scarce and almost all samples present μ values between 8 and 10 and κ values between 3.5 and 4.5 (insert graphs in Fig. 7).

4. Discussion

Since the mid 1970's many archaeological studies of metal provenance using lead isotope data were done on the basis of parallel analyses of geological and archaeological-metallurgical samples. This generated an important number of analytical data in different publications, some of them not always easy to find. Such a great amount of isotope data published in a variety of studies has been the subject of compilations subsequently used for metal provenance research. Nonetheless, and as signalled by different authors (e.g., Artioli et al., 2020; Cattin et al., 2009; Montero Ruiz, 2018; Radivojević et al., 2019), standardization of the data compiled is greatly needed in order to make such compilations a useful tool, in particular in archaeological studies but also in geochemical exploration for ore deposits. The utilization of an adequate programming language for statistical computing and generation of maps/graphics from the compiled data may further improve the result.

In this work a compilation of data from 140 different sources has been accomplished and different variables have been designed in order to allow for standardization and statistical treatment. A unique data file containing all the data and variables has been treated with the RStudio program for the calculations, plots and data pooling presented in this study. The combination of those two tools, database and statistical program, has enabled to create an interactive, user friendly website (www.ehu.eus/ibercron/iberlid) for data inspection, selection, generation of tables and representation on different graphs.

However, although the standardization of data is a basic requirement for a proper use of Pb isotope information with different purposes, such a large data compilation requires a critical study of the data themselves. In fact, statistics and graphs obtained by using IBERLID, like those presented in previous figures, show hardly explainable dispersion of values. This may be evidence of anomalous values and justifies a more detailed treatment of the values and data filtering to exclude outliers or spurious samples if needed. Thus, the dataset is discussed below on the basis of the variables established, including a proposal for data filtering and identification of outliers.

4.1. Pb isotope data of geological samples

The geological characteristics of the Iberian Peninsula have been used classically to define a number of main geological units or zones (e.g., Julivert et al., 1972). In the present case, sample location was the main variable used to establish groups of geological samples. Thus, following previous studies (e.g., Arribas, 1993; Lunar et al., 2002) and taking into account accepted zonal divisions for the geology of Iberia, we have established the 7 groups of geological samples previously mentioned (Fig. 2). These 7 groups show some common geological characteristics that are reflected in the isotopic ratios and parameters of the samples and are useful to search for and exclude anomalous values.

The anomalous dispersion observed for isotopic ratios of the samples from the northern branch of the Iberian Massif in comparison with those of all other geological areas considered (Fig. 5 and Table 2) appears to be directly related with a localized sampling area and the laboratory where the data were obtained (Álvarez Penales, 2016; Huelga-Suarez et al., 2014b, 2014a, 2012). All the isotope data of this group of geological samples show evidence of radiogenic Pb-bearing isotopic ratios, which points to high and variable U contents in the samples analysed, even within the same ore deposit. Apart from filtering the data of these samples, only few other samples have been discarded. This was effected because of: (i) the lack of $^{207}Pb/^{204}Pb$ ratio in the original work: sample code GDM.2042 from OXALID (Stos-Gale and Gale, 2009); and (ii) the anomalous relation between $^{206}Pb/^{204}Pb$ and $^{207}Pb/^{204}Pb$ ratios: sample codes GDM.0015 (Graeser and Friedrich, 1970), GDM.0020 (Doe, 1976), GDM.0031 (Dayton and Dayton, 1986), GDM.0057 (Brill et al., 1987) and GDM.2710 (Subías et al., 2015). The anomalous data for samples coded GDM.0069 to GDM.0080 are taken from Lillo (1992) quoting an internal report of ENADIMSA (1971). These data seem unreliable and the spread of values has been related to analytical problems (Canals and Cardellach, 1997) for which reason have been as well discarded from the database. The data for samples coded GDM.0213 to GDM.0227 also show a large dispersion, interpreted by the authors (Arias et al., 1996) as due to local radiogenic source in the basement. They have been also discarded as its inclusion would hinder the statistical use of the database.

Through this data filtering, the number of geological samples analysed is reduced from 1572 to 1458. As a result, there is a significant decrease in the dispersion of the isotopic ratios and in the anomalously low values of model ages obtained (Table A8).

In general, all the geological samples show as a common characteristic the existence of a relationship between the type of analysed material and the isotopic ratio obtained. Thus, when only model ages and μ values of galena samples are projected in 2D density diagrams grouped by geological zone, the relation between the geological zones defined and the isotopic ratios is patent (Fig. 8). Instead, the spread of isotopic ratios and related parameters drastically increases when Cu minerals are considered (Table A9). In detail, galena samples from the Betic Cordilleras show a bimodal distribution of model ages with a maximum at 90 Ma and other less representative peak around 360 Ma, which is consistent with the characteristics of the major geological units in the area. As for the μ values, they are nearly constant for all the samples of BC. In the post-Paleozoic Basque-Cantabrian Basin ore deposits, the samples show μ values of ca. 9.75 and model ages younger than 200 Ma, with a maximum at 140 Ma and a less representative peak around 50 Ma, in agreement with the geological characteristics of the basin, although the influence of 2 different sources of lead in the basement can not be discarded (Velasco et al., 1996). In the Catalonian Coastal Ranges region, the area defined by frequency of model age and μ values shows a unique maximum near 370 Ma, although with evident tendency to younger model ages as previously noted by (Canals and Cardellach, 1997) and attributed to local Pb source inhomogeneity. The cluster defined for the northern branch of the Iberian Massif (Fig. 8) shows a poorer definition and higher variation of μ values. An important maximum for this sector is defined around 320 Ma and a second one around 600 Ma. This, and the dispersion of μ values between 9.5 and 10.0 could indicate the influence of different Pb sources (Variscan and pre-Variscan), which would be consistent with the findings of late Precambrian to Ordovician magmatism there (Rubio-Ordóñez et al., 2015) but would require a more detailed study. The Ossa-Morena Zone shows the lowest values of μ pointing to an enhanced mantle contribution, not

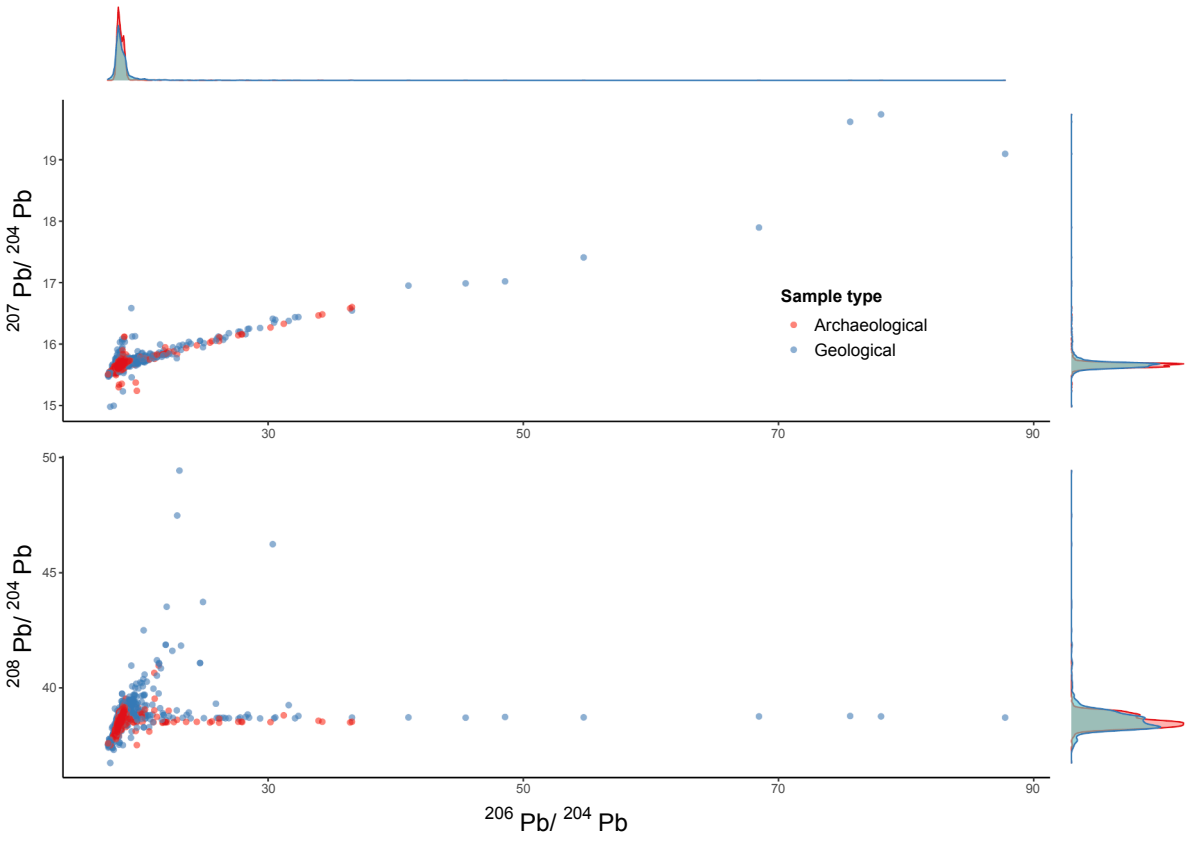

Fig. 4. Pb isotopic ratios of all samples included in the database and their statistical distribution for each main group proposed in the database: archaeological and geological samples.

detected in any other area in the Iberian Peninsula. On the other hand, model ages for the OMZ samples show a maximum at 350 Ma and two much less representative peaks around 420 and 610 Ma, all of it evidencing older mineralization events in the area and in good agreement with the geological characteristics of the Zone (see above). The 2D density distribution of analysed galena samples from the Pyrenees does not show clear peaks, with model ages spreading between 100 and 700 Ma, and μ values ranging from 9.63 to 10.20 (Fig. 8). The presence of this old Pb in the Alpine mountain range of the Pyrenees would be consistent with the occurrence there of a pre-Mesozoic basement, up to Ediacaran in age, affected by the Variscan and Alpine orogenies (Cardellach et al., 1996; García-Sansegundo et al., 2014). Finally, the peak defined in 2D density diagrams for the South Portuguese Zone shows a well defined maximum at 400 Ma and μ of 9.75, with poorly defined peaks towards lower μ values (<9.6) and older model ages (>600 Ma). These model ages are somewhat older than the mainly Devonian to lower Carboniferous metallogenic events described for the geology of the area (e.g., Barrie et al., 2002), and support the possible existence of a metallogenic event during the Cadomian orogeny (Marcoux et al., 2002).

While the relationship between isotopic characteristics of the Pb in galenas and the geological context appears to be clear, this correlation is impossible when all the ore samples compiled in IBERLID are considered. In fact, the inclusion of analyses of different minerals increases drastically the dispersion of isotope data and points to the incorporation of radiogenic lead (Table A9). A clear example is reflected for instance by the samples from the Ossa-Morena Zone. Galena samples from the OMZ define a very narrow cluster (Fig. 9, Table 4), but when all the ore samples are considered the dispersion increases significantly showing a continuous trend defined by the data of samples with different amounts of radiogenic Pb. The use of a variety of minerals bearing different U/Pb and Th/Pb ratios implies therefore that, even when the samples of a given restricted area are considered, the dispersion of isotopic ratios and related parameters prevents a proper definition of the lead isotopic characteristics of the area (Fig. 9, Table 4). Although radiogenic lead content is a classical tool for the absolute dating of geological materials and it has been recently applied in archaeological studies (Berger et al., 2019; Molofsky et al., 2014), the application of the lead isotopic analysis to radiogenic Pb-bearing archaeological samples implies that the common lead hypothesis is not valid and requires different methods for successful interpretations (Artioli et al., 2020; Killick et al., 2020).

4.2. *Pb isotope data from archaeological samples*

As mentioned above, a number of geological samples have been excluded from the compilation on the basis of their anomalous isotopic values, inconsistent with the geological characteristics of the Iberian Peninsula. While the same reasoning is not directly applicable to archaeological objects, a careful examination of the data for archaeological objects shows again a group of analyses with highly dispersed isotopic ratios, even when samples from a single location are considered (Álvarez Penales, 2016; Huelga-Suarez et al., 2014b; Reguera-Galan et al., 2019). For this reason, archaeological samples coded GDM.1327 (Huelga-Suarez et al., 2014b), GDM.2896 to GDM.2904 (Álvarez

Table 2
Statistical values obtained for: (A) all the geological samples included in IBERLID grouped by geological zone, and (B) only for galena samples.

Table 2A: Statistical values of isotopic ratios and related parameters for geological samples by geological zone.

Characteristic	BC, N = 324[1]	BCB, N = 33[1]	CCR, N = 106[1]	NIM, N = 535[1]	OMZ, N = 207[1]	Py, N = 88[1]	SPZ, N = 279[1]
$^{206}Pb/^{204}Pb$	18.70 (0.27), <17.63, >20.33	18.64 (0.08), <18.55, >18.76	18.60 (0.59), <18.30, >21.75	19.58 (6.04), <17.73, >87.76	18.77 (1.27), <17.44, >24.90	18.66 (1.39), <18.02, >30.36	18.32 (0.44), <17.49, >21.28
$^{207}Pb/^{204}Pb$	15.68 (0.06), <14.98, >15.80	15.66 (0.01), <15.62, >15.69	15.70 (0.03), <15.66, >15.86	15.73 (0.35), <15.23, >19.74	15.64 (0.09), <15.50, >16.05	15.71 (0.09), <15.58, >16.41	15.63 (0.04), <15.47, >15.78
$^{208}Pb/^{204}Pb$	38.85 (0.29), <36.74, >39.70	38.73 (0.05), <38.58, >38.85	38.65 (0.25), <37.53, >39.10	38.52 (0.34), <37.51, >40.97	38.71 (1.11), <37.37, >47.48	38.91 (1.48), <37.83, >49.43	38.36 (0.42), <37.41, >40.58
Model age (Ma)	85 (190), <-939, >482	108 (52), <-64, >181	207 (399), <-1,920, >527	-3,280 (24,396), <-223,237, >1,095	-55 (877), <-4,909, >898	141 (1,279), <-11,140, >749	291 (294), <-1,736, >706
μ	9.74 (0.58), <0.00, >10.27	9.73 (0.05), <9.54, >9.82	9.89 (0.08), <9.74, >10.33	10.15 (2.52), <8.14, >41.96	9.66 (0.24), <9.32, >11.32	9.96 (0.27), <9.50, >11.92	9.69 (0.10), <9.24, >10.08
k	3.94 (0.25), <0.00, >4.17	3.92 (0.04), <3.85, >3.99	3.94 (0.29), <2.61, >4.23	3.75 (0.74), <0.15, >4.90	3.85 (0.32), <2.27, >4.76	4.02 (0.29), <2.02, >5.26	3.93 (0.09), <3.31, >4.32

Table 2B: Statistical values of isotopic ratios and related parameters for galena samples by geological zone.

Characteristic	BC, N = 158[1]	BCB, N = 33[1]	CCR, N = 75[1]	NIM, N = 274[1]	OMZ, N = 52[1]	Py, N = 42[1]	SPZ, N = 37[1]
$^{206}Pb/^{204}Pb$	18.65 (0.19), <17.90, >18.89	18.64 (0.08), <18.55, >18.76	18.43 (0.12), <18.30, >18.68	18.22 (0.21), <17.73, >19.28	18.14 (0.16), <17.57, >18.51	18.35 (0.23), <18.02, >19.35	18.09 (0.25), <17.49, >18.38
$^{207}Pb/^{204}Pb$	15.68 (0.06), <15.00, >15.77	15.66 (0.01), <15.62, >15.69	15.69 (0.02), <15.66, >15.80	15.66 (0.09), <15.55, >16.59	15.60 (0.08), <15.51, >16.03	15.70 (0.04), <15.65, >15.87	15.62 (0.05), <15.47, >15.69
$^{208}Pb/^{204}Pb$	38.84 (0.25), <37.31, >39.19	38.73 (0.05), <38.58, >38.85	38.64 (0.28), <37.53, >39.10	38.41 (0.33), <37.67, >40.97	38.31 (0.25), <37.45, >39.13	38.56 (0.20), <38.16, >38.91	38.15 (0.25), <37.41, >38.40
Model age (Ma)	123 (156), <-935, >482	108 (52), <-64, >181	321 (79), <135, >527	402 (150), <58, >1,095	365 (120), <189, >898	383 (166), <-229, >749	432 (113), <209, >706
μ	9.72 (0.81), <0.00, >10.15	9.73 (0.05), <9.54, >9.82	9.89 (0.09), <9.74, >10.33	9.80 (0.35), <9.36, >13.42	9.61 (0.30), <9.33, >11.32	9.92 (0.16), <9.72, >10.66	9.67 (0.14), <9.24, >9.92
k	3.95 (0.33), <0.00, >4.17	3.92 (0.04), <3.85, >3.99	4.03 (0.11), <3.50, >4.23	4.03 (0.12), <3.74, >4.90	4.01 (0.09), <3.78, >4.29	4.04 (0.10), <3.51, >4.29	3.97 (0.05), <3.82, >4.13

[1] Statistics presented: mean (SD), <minimum, >maximum

[1] Statistics presented: mean (SD), <minimum, >maximum.

Penales, 2016) and GDM 2663-GDM.2688 (Reguera-Galan et al., 2019) have been filtered in IBERLID. Besides these, 7 more archaeological samples have been excluded due to their anomalous relation between $^{206}Pb/^{204}Pb$ and $^{207}Pb/^{204}Pb$, these are samples coded GDM.0477 (Stos-Gale, 2001), GDM.0023 (Craddock and Dauphas, 2011), GDM.2292 (Stos-Gale and Gale, 2009) and GDM.2438 to GDM.2441 (Mederos Martín et al., 2017).

As previously mentioned, in the case of archaeological samples the connection between geographical information and isotopic characteristics is not straightforward since there might be local or imported raw materials. The study of the type of object analysed and the lead isotope ratios and related parameters in archaeological samples is again a critical issue. In the present case, a distinct increase is observed for the so-called *Cu metal* samples, where $^{206}Pb/^{204}Pb$ ratios varies from 17.46 to 31.23; $^{207}Pb/^{204}Pb$ from 15.51 to 16.33 and $^{208}Pb/^{204}Pb$ from 37.51 to 40.97, as compared with the *Pb metal* samples ($^{206}Pb/^{204}Pb$, 18.07–18.84; $^{207}Pb/^{204}Pb$, 15.53–15.78; $^{208}Pb/^{204}Pb$, 38.02–39.34; Table A10). The wide Pb isotopic variations of archaeological Cu metals, mainly bronze samples, have been previously noted and sometimes attributed to the mix of materials with different isotopic composition employed in the metallurgy. However, as evidenced for the geological samples, when radiogenic lead is present the common lead hypothesis is

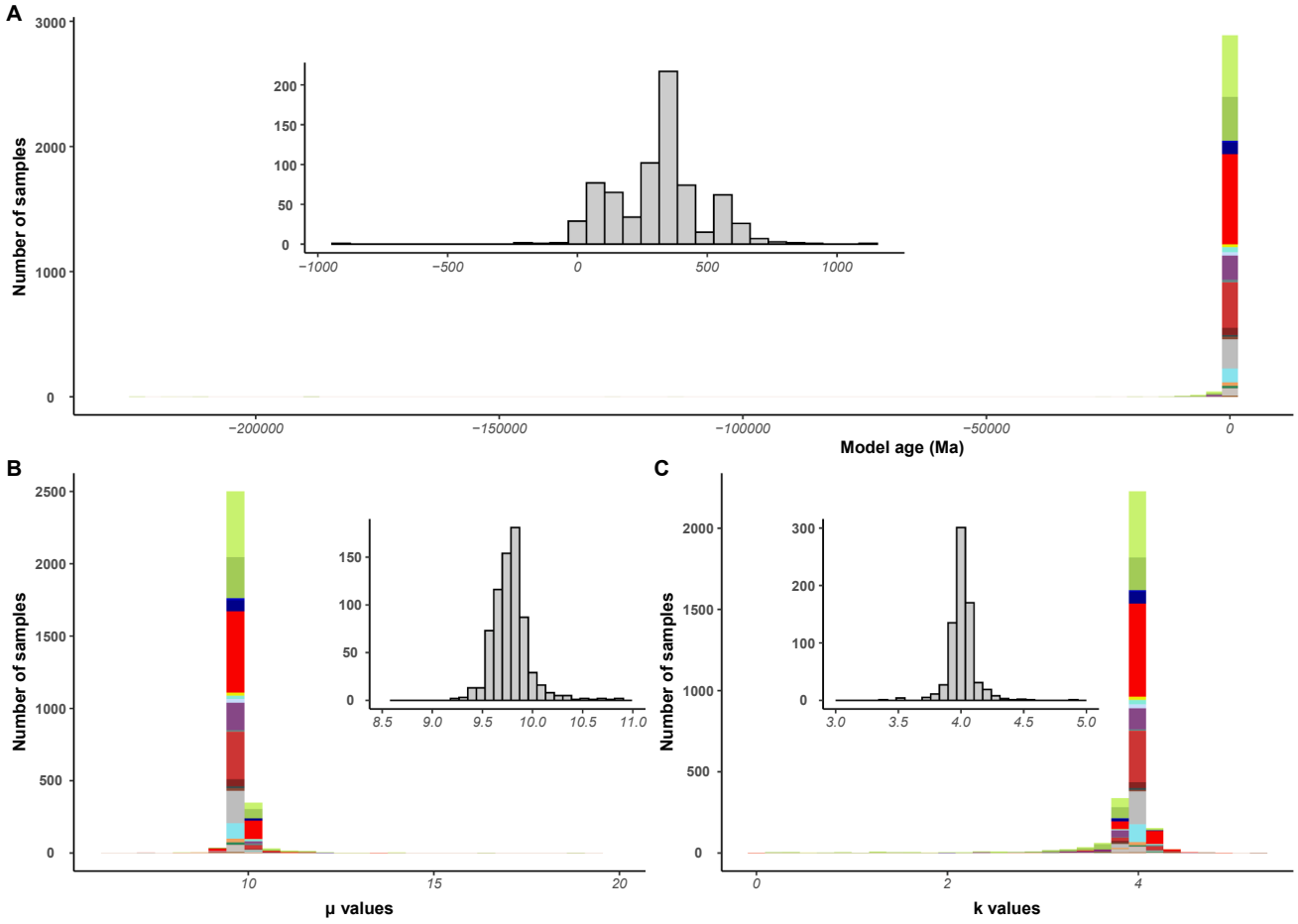

Fig. 5. Statistical distribution of A) Model ages (Ma), B) μ and C) κ obtained for all the samples and coloured by *analysed.material* (same colour code than Fig. 3); and only for galena in grey inserted graphs.

no longer valid. In those cases, isotopic ratios show much larger dispersions than when only common Pb is considered. In this situation, the application of alternative methods for data treatment has been proposed in archaeological studies (Artioli et al., 2020; Berger et al., 2019; Killick et al., 2020; Molofsky et al., 2014). The approach is similar to that in geochronological studies although the problem of common lead there is usually just the opposite since the presence of common Pb precludes the obtention of reliable ages. A typical strategy applied in geochronology for Pb correction can be useful to know the common Pb in radiogenic Pb-bearing samples. There are several methods for Pb correction (i.e. Andersen, 2002; Ludwig, 1999), although all of them involve the knowledge of U, Th and Pb contents in the analysed samples. If radiogenic lead contribution were corrected, at least for natural samples not subjected to metallurgical treatment that could change U/Pb and Th/Pb ratios, the real common Pb information could be obtained and the comparison with that of ore deposits could be more reliable. Unfortunately, the contents of those elements usually are not reported in publications dealing with lead isotopic ratios in archaeology. In our compilation <3% of the samples have U contents reported and in consequence this hypothesis cannot be adequately tested.

For a correct interpretation of the isotope results in archaeological samples, Pernicka (2014) and other authors have recommended to use the trace element concentrations besides the lead isotopic data. The use of the trace element analyses could be useful in two different ways: (i) as a combination of geochemical tracers, and (ii) through the correction as indicated of lead isotopic ratios on the basis of the U, Th and Pb concentrations in the samples. In fact, classical and recent studies include also lead isotopic ratios and elemental analyses of archaeological samples (e.g. Nocete et al., 2018; Stos-Gale et al., 1999) and this is becoming more common in the last years. Unfortunately, the lack of standardization for trace elements is even worse than in the case of the lead isotopic analyses. The disparities in elemental analyses are related to the different analytical techniques employed, accurate and precision of data, and quantified analytes that may be highly variable even for the same type of samples (e.g., 21 analytes in Nocete et al., 2018, determined by laser ablation techniques, vs. 7 elements by X-Ray fluorescence in Stos-Gale et al., 1999), all of which greatly complicates at present the comparison among samples. The inclusion of elemental concentrations in a database as IBERLID would greatly increase the possibilities of the tool but, although the design of both database and statistical software would allow such update, it would require an intensive project including many thousands of elemental data an exhaustive work of data compilation and standardization.

4.3. *On the source of Pb in geological samples*

The use of comprehensive datasets, together with suitable variables, data grouping, filtering and finally selected values allows fot statistical

Table 3
Statistical values obtained for all the archaeological samples included in IBERLID grouped by the type of analysed material.

Characteristic	Cu metal, N = 525[1]	Cu mineral, N = 16[1]	Fe metal, N = 14[1]	Galena, N = 50[1]	Gold, N = 21[1]	Hg mineral, N = 6[1]	Litharge, N = 27[1]	Ore mix, N = 2[1]	Pb, N = 4[1]	Pb metal, N = 360[1]	Pb mineral, N = 5[1]	Silver, N = 230[1]	Slag, N = 110[1]	Sn metal, N = 30[1]	unk, N = 5[1]
$^{206}Pb/^{204}Pb$	18.88 (2.02), <17.46, >36.57	18.83 (0.61), <18.28, >20.13	18.56 (0.14), <18.38, >18.78	18.39 (0.16), <18.28, >18.78	18.32 (0.16), <17.99, >18.62	18.52 (0.14), <18.36, >18.71	18.47 (0.29), <18.08, >18.74	18.40 (0.06), <18.36, >18.45	18.30 (0.01), <18.29, >18.30	18.41 (0.21), <18.07, >18.84	19.28 (0.64), <18.42, >20.04	18.45 (0.23), <18.12, >18.86	18.27 (0.08), <18.16, >18.43	18.65 (0.31), <18.23, >19.71	18.07 (0.26), <17.85, >18.38
$^{207}Pb/^{204}Pb$	15.68 (0.11), <15.30, >16.60	15.67 (0.04), <15.62, >15.77	15.67 (0.01), <15.66, >15.69	15.68 (0.03), <15.60, >15.80	15.64 (0.03), <15.58, >15.68	15.68 (0.03), <15.65, >15.72	15.65 (0.06), <15.49, >15.70	15.66 (0.04), <15.63, >15.69	15.68 (0.00), <15.67, >15.68	15.65 (0.05), <15.53, >16.12	15.70 (0.06), <15.64, >15.79	15.65 (0.03), <15.58, >15.83	15.64 (0.02), <15.59, >15.75	15.58 (0.10), <15.24, >15.66	15.61 (0.02), <15.59, >15.64
$^{208}Pb/^{204}Pb$	38.58 (0.28), <37.51, >40.97	38.60 (0.19), <38.34, >38.92	38.65 (0.09), <38.48, >38.82	38.59 (0.21), <38.28, >39.15	38.41 (0.22), <38.00, >38.88	38.68 (0.25), <38.38, >39.09	38.62 (0.48), <37.77, >39.10	38.55 (0.04), <38.52, >38.58	38.53 (0.02), <38.50, >38.54	38.58 (0.28), <38.02, >39.34	38.70 (0.22), <38.40, >38.93	38.61 (0.27), <37.98, >39.54	38.38 (0.14), <38.15, >38.80	38.58 (0.32), <37.52, >38.99	38.16 (0.32), <37.90, >38.62
Model age (Ma)	−1695 (19260), <-222911, >706	−26 (385), <-821, >371	178 (89), <26, >295	323 (93), <91, >527	303 (85), <164, >500	223 (97), <90, >356	213 (136), <69, >436	278 (121), <193, >364	389 (6), <381, >392	259 (136), <-17, >812	−316 (518), <-788, >495	234 (125), <-13, >460	346 (43), <247, >446	−94 (481), <-2044, >247	436 (152), <235, >568
μ	9.82 (0.40), <8.41, >14.14	9.72 (0.10), <9.59, >9.93	9.77 (0.03), <9.71, >9.82	9.84 (0.11), <9.56, >10.33	9.70 (0.08), <9.51, >9.82	9.80 (0.11), <9.71, >9.94	9.72 (0.17), <9.19, >9.89	9.77 (0.18), <9.65, >9.89	9.86 (0.02), <9.83, >9.87	9.74 (0.19), <9.30, >11.57	9.78 (0.29), <9.59, >10.27	9.74 (0.10), <9.45, >10.33	9.73 (0.08), <9.55, >10.13	9.42 (0.40), <8.11, >9.72	9.66 (0.04), <9.64, >9.73
κ	3.83 (0.54), <0.44, >4.23	3.77 (0.29), <3.15, >4.02	3.94 (0.07), <3.81, >4.01	4.02 (0.04), <3.91, >4.23	3.96 (0.05), <3.87, >4.05	3.98 (0.10), <3.85, >4.11	3.97 (0.09), <3.73, >4.06	3.99 (0.08), <3.93, >4.04	4.05 (0.01), <4.04, >4.06	3.99 (0.07), <3.83, >4.29	3.56 (0.38), <3.27, >4.20	3.98 (0.06), <3.79, >4.25	3.98 (0.04), <3.91, >4.15	3.82 (0.29), <2.64, >4.01	3.99 (0.07), <3.89, >4.08

[1]Statistics presented: mean (SD), <minimum, >maximum.

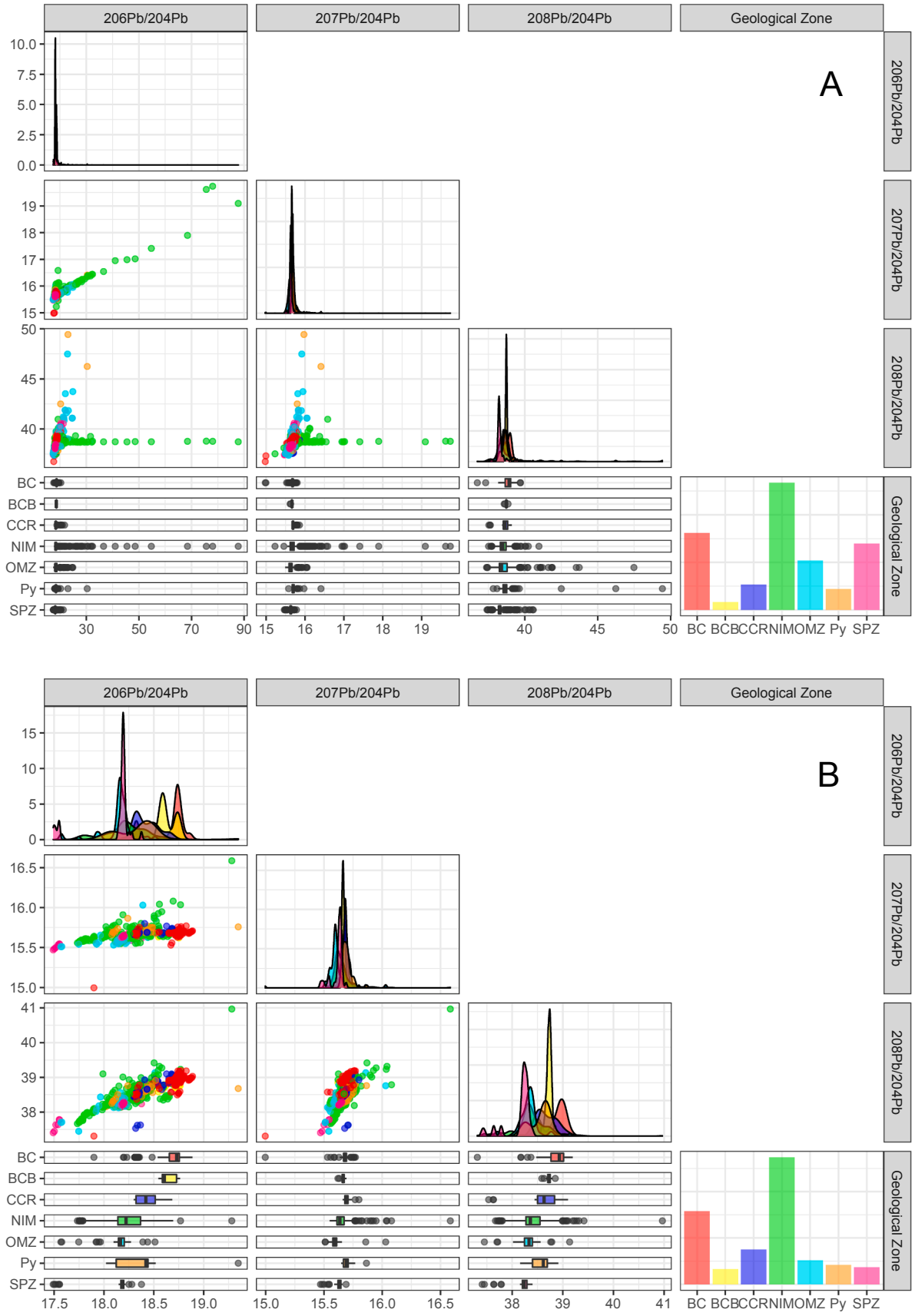

Fig. 6. Scatter diagrams of isotopic ratios grouped by geological zones for (A) all the geological samples and (B) only samples of galena. Colour code in Fig. 2.

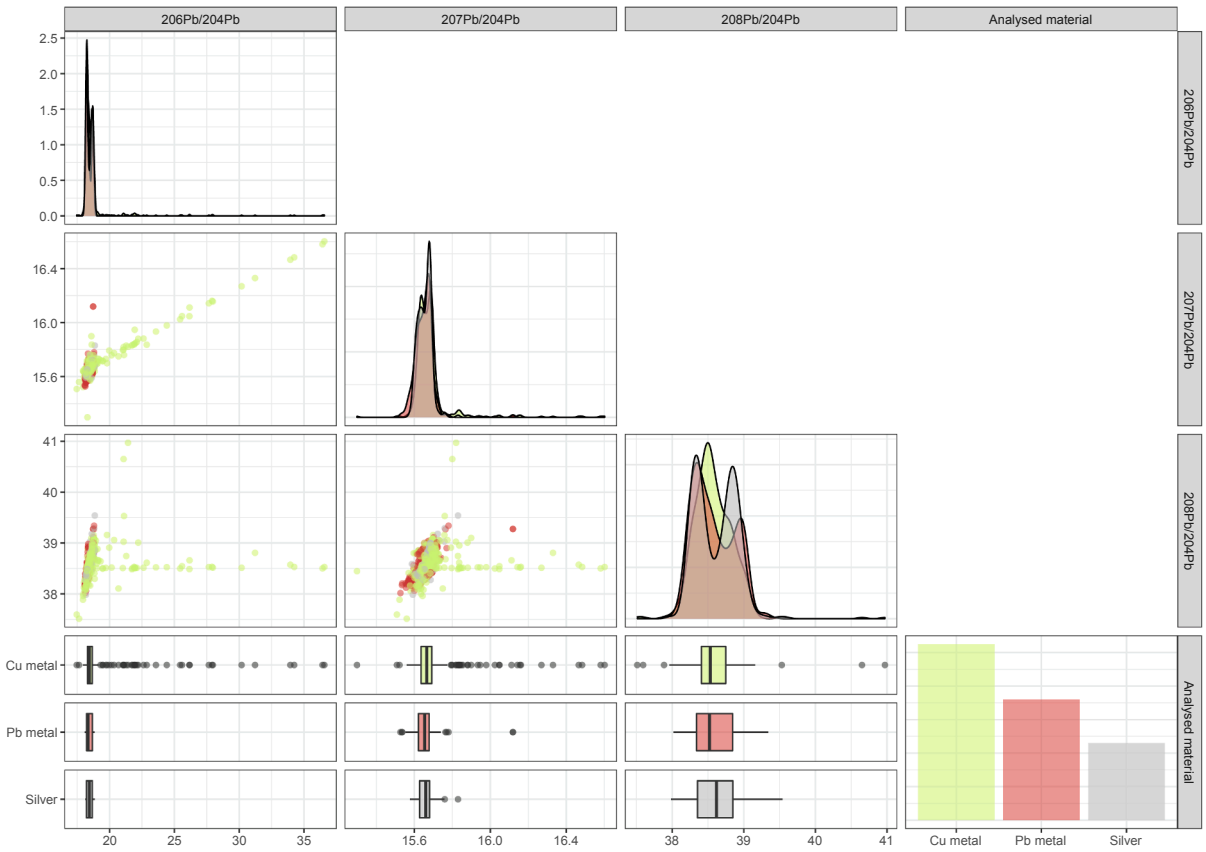

Fig. 7. Scatter diagrams of isotopic ratios grouped by analysed materials for all the archaeological samples. Only the 3 more abundant species of analysed materials are considered. Colour code in Fig. 3.

treatment and data interpolation. The maps of Fig. 10 reflect the isotopic characteristics of Pb in the Iberian Peninsula and Balearic Islands obtained by interpolation of geolocalised Pb isotope ratios and parameters. To this effect, after discarding spurious results, the data compiled in IBERLID for galena samples, were interpolated by ordinary kriging of block mean values using inverse distance weighted interpolation (Cressie, 1993). The interpolation of data defines a distinctive lead isotopic area in the Ossa-Morena Zone with higher model ages, older than 500 Ma (Fig. 10A), that point to the existence of a Cadomian metallogenic event (Marcoux et al., 2002), and low values of μ, below 9.6 (Fig. 10B), whereby some kind of mantellic participation can be suspected. On the other hand, the interpolation shows the presence of 2 different isotopic compositions in the Betic System (Fig. 10A), with model ages between 200 and 400 Ma in the west of Cabo de Gata and mainly between 0 and 100 Ma to the east of this site. However, μ values for all the samples in this area show high values, always > 9.7 (Fig. 10B). The relationship between κ values and the geological setting is not evident and the interpolation obtained using κ values of galena samples displays an unclear distribution (Fig. 10C) This suggests changes in the Th/U ratios through geological time even in the mantle, presumably because of the differences in U and Th solubility and oxidation states (Elliott et al., 1999).

5. Geological implications of the database and tool

Lead isotope geochemistry has played a vital role in tracing the fluid pathways and sources of metal in ore deposits, allowing for chronological information of ore body formation and evaluation of the economic potential in ore exploration (e.g., Arribas and Tosdal, 1994; Hsu et al., 2019). In this sense, the use of the compiled Pb isotopic ratios from ore deposits and of their spatial location, combined with the statistical treatment enabled by the IBERLID or ad hoc tools allow to establish informed and extended interpretations on Iberian metallogenic provinces, their ages and formation events. The interpolated maps of Pb isotope related parameters of the Iberian Peninsula and Balearic Islands (Fig. 10) reflect a direct relation between major geological units in the area and their isotopic characteristics.

The statistical application of Pb isotopic data compiled in the database allows to establish a plumbotectonic model for the Iberian realm. Thus, all the ore deposits comprised in the IBERLID compilation show model ages younger than ca. 600 Ma (Figs. 5, 8 and 10) and define 3 main events of ore formation: (1) a Neoproterozoic to Cambrian event around 600 Ma mainly situated within terranes of the Ossa-Morena Zone; it is characterized by μ values lower than 9.4 and would be compatible with the development of arc units during the Cadomian orogeny, with local influence of mantle-related mineralizations as described in previous studies (e.g., Tornos and Chiaradia, 2004); (2) an Upper Paleozoic second event around 300 Ma is present through all the Iberian realm being specially well represented in the Central Iberian and Ossa-Morena Zones, and also within the axial zone of the Pyrenean Cordillera; these Variscan s.l. mineralizations display distinctive crustal μ values mainly between 9.6 and 9.8 that could originate as a result of direct leaching of pre-Variscan sediments probably extracted at various times (Arribas, 1993; Palero-Fernández et al., 2015); finally (3) a

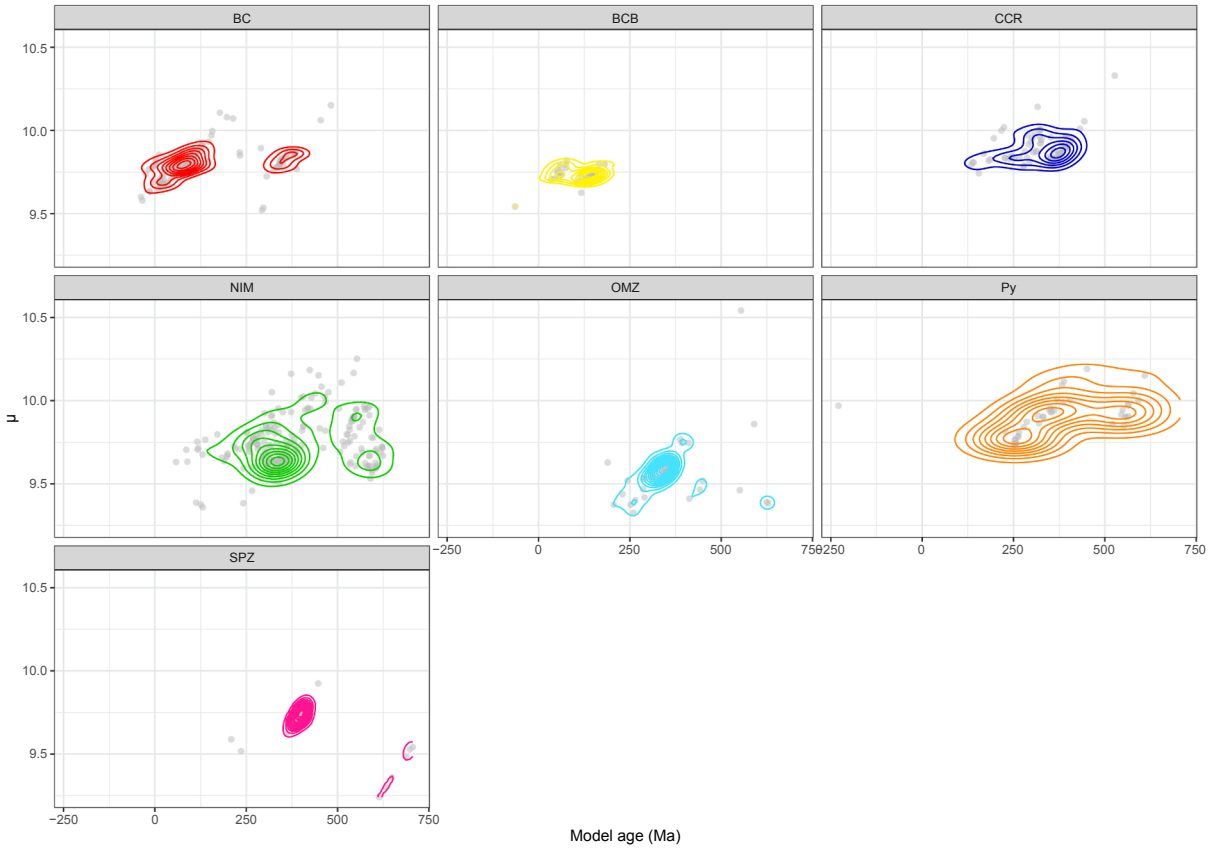

Fig. 8. 2D density diagrams for model ages (Ma) versus μ for galena samples grouped by geological zones. Grey points are all the data of each zone. Colour code in Fig. 2.

younger event, geographically limited to the Betic System and Basque Cantabrian Basin, corresponds to ore deposits with crustal μ values around 9.7 and would be related to events of the late Mesozoic to the Neogene Alpine Orogeny and volcanic activity (Arribas and Tosdal, 1994).

6. Conclusions

The IBERLID database presented includes Pb isotope ratios for a high number of geological and archaeological samples, and additional geographical and geological information on the samples. This allows the intercomparison of Pb isotope ratios and a conscious use of the compiled data to link a lead isotopic signature to a specific mining district.

Major difficulties in the compilation result of: (i) proper data assessment due to the lack of errors and analytical information in published values, (ii) accuracy of sample location due to insufficient information, and (iii) standardization of variables to configure a usable database. Upon solving these problems as best as possible trough exhaustive bibliographic revision and prudent simplification of the variables considered, the use of RStudio programming language for statistical computing and graphics enabled the design of a tool to obtain reproducible graphs with multiple data pooling options. Different types of graphs and tables shown as examples in Figs. 2 to 10, Tables 2 to 4 and Supplementary Tables A1 to A10 demonstrate the capability of the tool. IBERLID is an open database accessible through a web site (www.ehu.eus/ibercron/iberlid) designed with the same software, which will permit the scientific community to get basic graphs and select data in a friendly way.

Lead isotopic analysis (LIA) has been an increasingly used tool in geological studies of ore deposits and in archaeological studies of metal provenance during the last 6 decades. This permitted the compilation of data for nearly 3000 samples from the Iberian Peninsula and Balearic Islands contained in 140 publications referenced in the supplementary material. The IBERLID database includes these results reducing difficulties associated to the comparison of isotopic data from less complete datasets.

Lead isotope ratios of geological samples from the Iberian realm show a clear relationship to 3 main processes of ore genesis. The processes were related to main orogenic events during three different moments of the geological history: (1) Cadomian events in the Ossa-Morena Zone, (2) Variscan mineralizations through all the area excepting the Basque-Cantabrian Basin, and (3) Alpine deposits, located in the Pyrenees and Betic Cordilleras. Each of these events is characterized by distinctive lead isotope ratios consistent with the geological attributes of the ore deposits. Yet, the incorporation sometimes of radiogenic lead hinders the interpretation of some data. The geological, geographical and mineralogical standardized information compiled in IBERLID allows to discern isotope differences even within the same ore deposit.

Model ages, μ and κ parameters are included in the database. These are useful tools to discern among samples with similar isotope ratios and easily allow to detect radiogenic-Pb bearing samples. Lead isotope maps for the Iberian realm are presented for the first time. They evidence the relationship between Pb isotope attributes and the geology of this domain, and support the validity of IBERLID in metallogenic research.

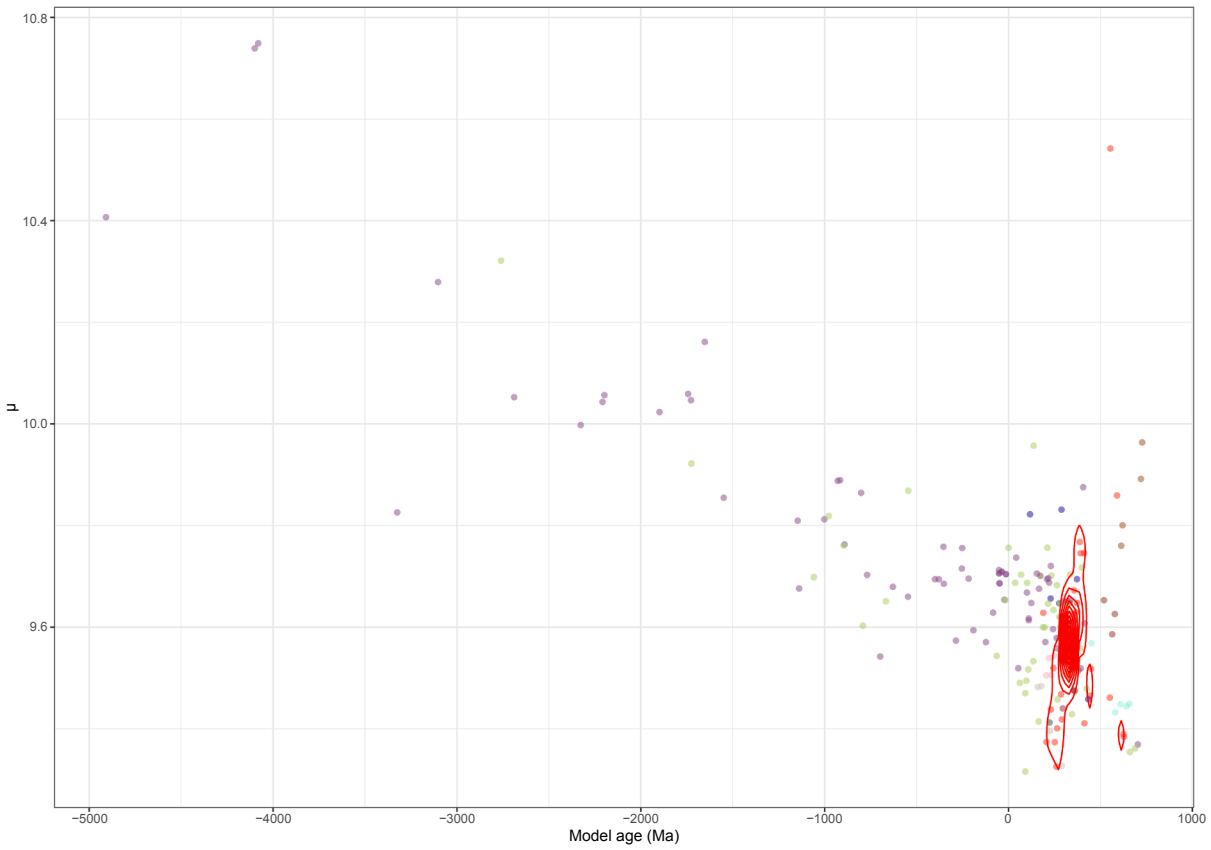

Fig. 9. Comparison between galena and other analysed minerals of the Ossa-Morena Zone. In red, cluster obtained for galena. The points represent individual analyses of OMZ. Legend of colours is the same as in Fig. 3.

Table 4
Statistical values obtained for geological samples from Ossa-Morena Zone (OMZ) grouped by the type of analysed material.

Characteristic	Cu mineral, N = 47[1]	Fe mineral, N = 6[1]	Galena, N = 51[1]	Gold, N = 1[1]	Hg mineral, N = 5[1]	Ore mix, N = 75[1]	Pb mineral, N = 8[1]	Sb mineral, N = 2[1]	W mineral, N = 4[1]	Whole rock, N = 4[1]	Zn mineral, N = 4[1]
$^{206}Pb/^{204}Pb$	18.71 (0.96), <17.46, >22.88	18.33 (0.26), <17.93, >18.70	18.14 (0.16), <17.57, >18.51	18.52 (NA), <18.52, >18.52	17.69 (0.17), <17.57, >17.98	19.56 (1.66), <17.44, >24.90	18.01 (0.15), <17.81, >18.23	18.20 (0.02), <18.19, >18.22	18.30 (0.02), <18.28, >18.32	18.24 (0.15), <18.05, >18.37	17.83 (0.05), <17.77, >17.87
$^{207}Pb/^{204}Pb$	15.63 (0.07), <15.50, >15.92	15.64 (0.05), <15.55, >15.69	15.60 (0.05), <15.51, >15.86	15.65 (NA), <15.65, >15.65	15.54 (0.03), <15.53, >15.58	15.69 (0.10), <15.50, >16.05	15.58 (0.02), <15.56, >15.62	15.57 (0.02), <15.56, >15.59	15.59 (0.01), <15.59, >15.60	15.56 (0.03), <15.53, >15.59	15.64 (0.02), <15.62, >15.67
$^{208}Pb/^{204}Pb$	38.71 (1.43), <37.53, >47.48	38.47 (0.29), <38.03, >38.93	38.30 (0.24), <37.45, >39.13	38.50 (NA), <38.50, >38.50	37.77 (0.17), <37.65, >38.06	39.26 (1.22), <37.54, >43.73	38.03 (0.40), <37.37, >38.39	38.18 (0.08), <38.12, >38.24	38.40 (0.05), <38.33, >38.46	38.01 (0.11), <37.87, >38.12	37.95 (0.38), <37.61, >38.31
Model age (Ma)	−8 (624), <-2760, >688	286 (110), <117, >433	355 (94), <189, >628	173 (NA), <173, >173	587 (82), <451, >657	−572 (1178), <-4909, >703	423 (112), <295, >578	264 (58), <223, >305	226 (18), <206, >248	213 (58), <159, >290	670 (62), <613, >727
μ	9.63 (0.17), <9.32, >10.32	9.68 (0.14), <9.46, >9.83	9.57 (0.17), <9.33, >10.54	9.70 (NA), <9.70, >9.70	9.47 (0.06), <9.43, >9.57	9.76 (0.24), <9.37, >10.75	9.55 (0.09), <9.44, >9.65	9.48 (0.09), <9.41, >9.54	9.52 (0.02), <9.51, >9.54	9.42 (0.08), <9.33, >9.48	9.85 (0.09), <9.76, >9.96
κ	3.86 (0.29), <2.90, >4.76	3.98 (0.06), <3.91, >4.10	4.01 (0.08), <3.78, >4.29	3.88 (NA), <3.88, >3.88	4.01 (0.02), <3.99, >4.03	3.68 (0.40), <2.27, >4.49	3.94 (0.15), <3.70, >4.12	3.89 (0.07), <3.84, >3.94	3.95 (0.02), <3.93, >3.97	3.77 (0.03), <3.75, >3.81	4.06 (0.26), <3.82, >4.29

[1] Statistics presented: mean (SD), <minimum, >maximum.

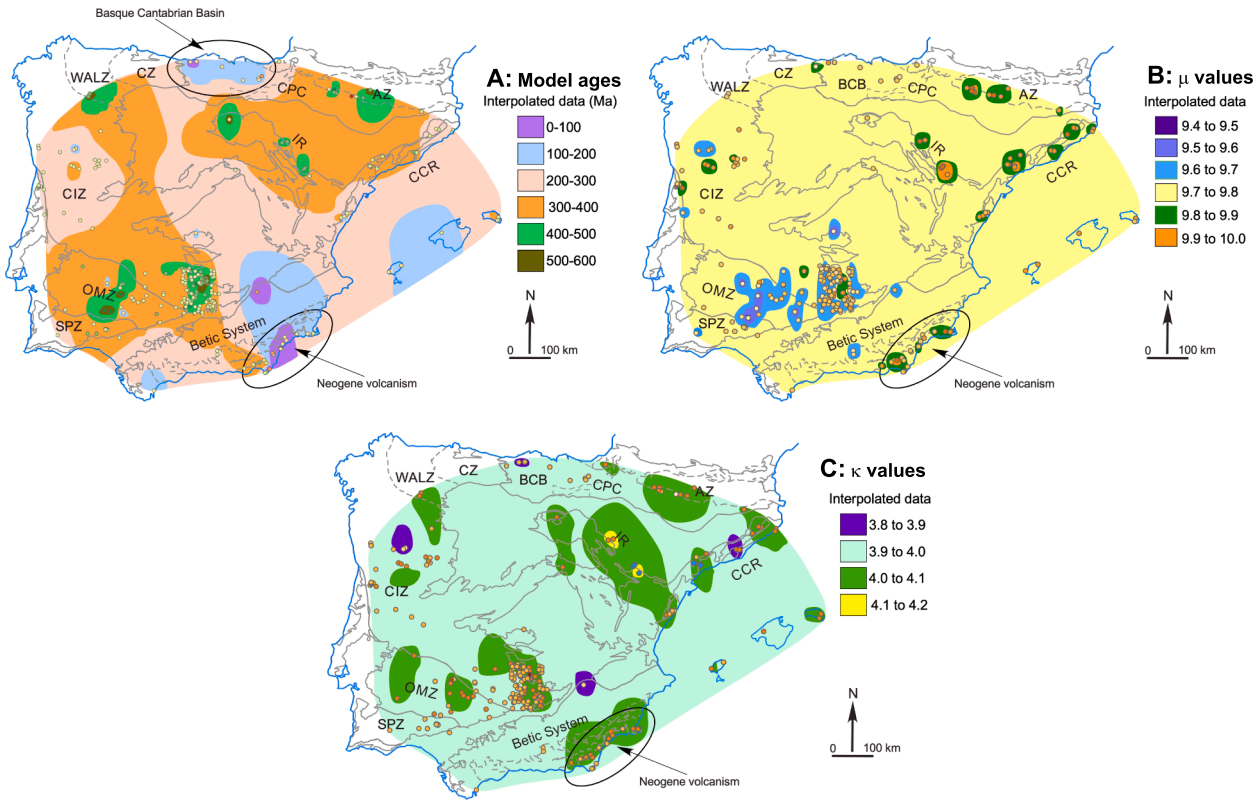

Fig. 10. Interpolated maps for Pb isotopic characteristics of the Iberian Peninsula. Data of individual samples are shown as dots with different colour based on their individual values. Coloured areas are obtained by interpolation (see text). Each map includes a: model ages; b: μ values; c: κ values; and d: location of main geological zones considered in the Iberian Peninsula.

By using the same standardization scheme to maintain the ability for sample grouping and comparison, the database allows the addition of results from new samples or even new variables, e.g. elemental analyses, that might increase the productivity of the tool.

Declaration of Competing Interest

The authors declare that they have no known competing financial interests or personal relationships that could have appeared to influence the work reported in this paper.

Acknowledgments

Financial support was provided by the Spanish Ministry of Economy, Industry and Competitiveness, and the European Regional Development Fund (MINECO/ERDF CGL2015- 63530-P), and by the UPV/EHU (GIU15/05). The authors are grateful to Sabine Klein and two anonymous reviewers for constructive comments which improved this manuscript, and to Huayong Chen for suggestions and editorial handling.

Appendix A. Supplementary data

Supplementary data to this article can be found online at https://doi.org/10.1016/j.oregeorev.2021.104279.

References

Albarède, F., Blichert-Toft, J., Rivoal, M., Telouk, P., 2016. A glimpse into the Roman finances of the Second Punic War through silver isotopes. Geochemical Perspect. Lett. 2, 127–137. https://doi.org/10.7185/geochemlet.1613.

Albarède, F., Desaulty, A.-M.-M., Blichert-Toft, J., 2012. A geological perspective on the use of Pb isotopes in archaeometry. Archaeometry 54, 853–867. https://doi.org/10.1111/j.1475-4754.2011.00653.x.

Allègre, C.J., 2008. In: Isotope Geology. Cambridge University Press, Cambridge.

Álvarez Penales, P., 2016. Medida de relaciones isotópicas de plomo en muestras arqueológicas mediante MC-ICP-MS. Universidad de Oviedo.

Andersen, M.B., Stirling, C.H., Weyer, S., 2017. Uranium isotope fractionation, in: Non-Traditional Stable Isotopes. Walter de Gruyter GmbH, pp. 799–850. https://doi.org/10.2138/rmg.2017.82.19.

Andersen, T., 2002. Correction of common lead in U-Pb analyses that do not report 204Pb. Chem. Geol. 192 (1-2), 59–79. https://doi.org/10.1016/S0009-2541(02)00195-X.

Arias, D., Corretge, L.G., Suarez, O., Villa, L., Cuesta, A., Gallastegui, G., 1996. Lead and sulfur isotope compositions of the Ibias gold vein system (NW Spain); genetic implications. Econ. Geol. 91, 1292–1297. https://doi.org/10.2113/gsecongeo.91.7.1292.

Arribas, A., 1993. Observations on the isotopic composition of ore Pb in the Iberian Peninsula, in: Fenoll, P., Torres, J., Gervilla, F. (Eds.), Current Research in Geology Applied to Ore Deposit. pp. 29–32.

Arribas, A., Tosdal, R.M., 1994. Isotopic composition of Pb in ore deposits of the Betic Cordillera Spain: origin and relationship to other European deposits. Econ. Geol. 89, 1074–1093. https://doi.org/10.2113/gsecongeo.89.5.1074.

Artioli, G., Angelini, I., Nimis, P., Villa, I.M., 2016. A lead-isotope database of copper ores from the Southeastern Alps: A tool for the investigation of prehistoric copper metallurgy. J. Archaeol. Sci. 75, 27–39. https://doi.org/10.1016/j.jas.2016.09.005.

Artioli, G., Canovaro, C., Nimis, P., Angelini, I., 2020. LIA of Prehistoric Metals in the Central Mediterranean Area: A Review. Archaeometry 62, 53–85. https://doi.org/10.1111/arcm.12542.

Barrie, T.C., Amelin, Y., Pascual, E., 2002. U-Pb geochronology of VMS mineralization in the Iberian Pyrite belt. Miner. Depos. 37 (8), 684–703. https://doi.org/10.1007/s00126-002-0302-7.

Bell, K., Franklin, J.M., 1993. Application of lead isotopes to mineral exploration in glaciated terrains. Geology 21, 1143–1146. https://doi.org/10.1130/0091-7613(1993)021<1143:AOLITM>2.3.CO;2.

Berger, D., Soles, J.S., Giumlia-Mair, A.R., Brügmann, G., Galili, E., Lockhoff, N., Pernicka, E., Zerboni, A., 2019. Isotope systematics and chemical composition of tin ingots from Mochlos (Crete) and other Late Bronze Age sites in the eastern Mediterranean Sea: An ultimate key to tin provenance? PLoS One 14 (6), e0218326. https://doi.org/10.1371/journal.pone.0218326.

Birch, T., Westner, K.J., Kemmers, F., Klein, S., Höfer, H.E., Seitz, H.-M., 2020. Retracing Magna Graecia's silver: coupling lead isotopes with a multi-standard trace element procedure. Archaeometry 62 (1), 81–108. https://doi.org/10.1111/arcm.12499.

Brill, R.H., Barnes, I.L., Tong, S.C., Joel, E.C., Murtaugh, M.J., 1987. Laboratory studies of some European artifacts excavated on San Salvador Island, in: Gerace, D. (Ed.),

Columbus and His World: Proceedings of the First San Salvador Conference. San Salvador, Bahamian Field Station, pp. 247–292.
Brill, R.H., Wampler, J., 1967. Isotope ratios in archaeological objects of lead, in: Young, W. (Ed.), Application of Science in Examination of Works of Art. Museum of Fine Arts, Boston, pp. 155–66.
Canals, A., Cardellach, E., 1997. Ore lead and sulphur isotope pattern from the low-temperature veins of the Catalonian Coastal Ranges (NE Spain). Miner. Depos. 32 (3), 243–249. https://doi.org/10.1007/s001260050089.
Cannon, R.S., Pierce, A.P., 1969. Lead isotope guides for Mississippi Valley lead-zinc exploration. Contrib. to Econ. Geol. Geol. Surv. Bull. 1312-G, 20. https://doi.org/10.3133/b1312G.
Cardellach, E., Canals, A., Pujals, I., 1996. La composicion isotopica del azufre y del plomo en las mineralizaciones de Zn-Pb del valle de Aran (Pirineo Central) y su significado metalogenetico. Estud. Geol. 52 (5–6) https://doi.org/10.3989/egeol.96525-6.
Cattin, F., Guénette-Beck, B., Besse, M., Serneels, V., 2009. Lead isotopes and archaeometallurgy. Archaeol. Anthropol. Sci. 1 (3), 137–148. https://doi.org/10.1007/s12520-009-0013-4.
Craddock, P.R., Dauphas, N., 2011. Iron Isotopic Compositions of Geological Reference Materials and Chondrites. Geostand. Geoanalytical Res. 35, 101–123. https://doi.org/10.1111/j.1751-908X.2010.00085.x.
Cressie, N.A.C., 1993. Statistics for Spatial Data, Journal of Agricultural, Biological, and Environmental Statistics, Wiley Series in Probability and Statistics. John Wiley & Sons, Inc., Hoboken, NJ, USA. https://doi.org/10.1002/9781119115151.
Dallmeyer, R.D., Martínez García, E. (Eds.), 1990. Pre-Mesozoic Geology of Iberia, Pre-Mesozoic Geology of Iberia. Springer Berlin Heidelberg. https://doi.org/10.1007/978-3-642-83980-1.
Dayton, J.E., Dayton, A., 1986. Uses and Limitations of Lead Isotopes in Archaeology. In: Olin, J.S., Blackman, M.J. (Eds.), Proceedings of the 24th International Archaemetry Symposium, pp. 13–41.
Desaulty, A.-M., Telouk, P., Albalat, E., Albarede, F., 2011. Isotopic Ag-Cu-Pb record of silver circulation through 16th-18th century Spain. Proc. Natl. Acad. Sci. U. S. A. 108 (22), 9002–9007. https://doi.org/10.1073/pnas.1018210108.
Dickin, A.P., 2018. Radiogenic Isotope Geology, 3rd ed. Cambridge University Press, Cambridge. https://doi.org/10.1017/9781316163009.
Doe, B.R., 1976. Lead Isotope Data Bank: 2,624 Samples and Analyses Cited. USGS Open-File Report 76–201.
Elliott, Tim, Zindler, Alan, Bourdon, Bernard, 1999. Exploring the kappa conundrum: The role of recycling in the lead isotope evolution of the mantle. Earth Planet. Sci. Lett. 169 (1-2), 129–145. https://doi.org/10.1016/S0012-821X(99)00077-1.
ENADIMSA, 1971. Investigación minera en Linares: Fase previa de trabajos básicos. Unpublished internal report, II.Estudios metalogénicos.
Gale, N.H., 2009. A response to the paper of A.M. Pollard:, in: Shortland, A.J., Freestone, I.C., Rehren, T. (Eds.), From Mine to Microscope, Advances in the Study of Ancient Technology. Oxbow Books, pp. 191–196.
García-Sansegundo, J., Martin-Izard, A., Gavaldà, J., 2014. Structural control and geological significance of the Zn-Pb ores formed in the Benasque Pass area (Central Pyrenees) during the post-late Ordovician extensional event of the Gondwana margin. Ore Geol. Rev. 56, 516–527. https://doi.org/10.1016/j.oregeorev.2013.06.001.
Gibbons, W., Moreno, T. (Eds.), 2002. The Geology of Spain. The Geological Society of London.
Graeser, Stefan, Friedrich, Günther, 1970. Zur Frage der Altersstellung und Genese der Blei-Zink-Vorkommen der Sierra de Cartagena in Spanien. Miner. Depos. 5 (4), 365–374. https://doi.org/10.1007/BF00206733.
Gulson, B.L., 1986. Lead Isotopes in Mineral Exploration., Developments in Economic Geology Series. Elsevier. https://doi.org/10.1017/S001675680000964X.
Higueras, Pablo, Munhá, José, Oyarzun, Roberto, Tassinari, Colombo C.G., Ruiz, Izabel R., 2005. First lead isotopic data for cinnabar in the Almadén district (Spain): Implications for the genesis of the mercury deposits. Miner. Depos. 40 (1), 115–122. https://doi.org/10.1007/s00126-005-0471-2.
Holk, Gregory J, Kyser, T.Kurtis, Chipley, Don, Hiatt, Eric E, Marlatt, Jim, 2003. Mobile Pb-isotopes in Proterozoic sedimentary basins as guides for exploration of uranium deposits. J. Geochemical Explor. 80 (2-3), 297–320. https://doi.org/10.1016/S0375-6742(03)00196-1.
Hsu, Yiu-Kang, Sabatini, Benjamin J., Xia, Qun-Ke, 2019. A geochemical characterization of lead ores in China: An isotope database for provenancing archaeological materials. PLoS One 14 (4), e0215973. https://doi.org/10.1371/journal.pone.0215973.
Huelga-Suarez, G., Moldovan, M., Suárez Fernández, M., Ángel De Blas Cortina, M., Ignacio García Alonso, J., 2014a. Defining the lead isotopic fingerprint of copper ores from north-west Spain: The El Milagro Mine (Asturias). Archaeometry 56, 88–101. https://doi.org/10.1111/arcm.12005.
Huelga-Suarez, G., Moldovan, M., Suárez Fernández, M., de Blas Cortina, M. Ángel, García Alonso, J.I., 2014b. Isotopic composition of lead in copper ores and a copper artefact from the La profunda mine (León, Spain). Archaeometry 56 (4), 651–664. https://doi.org/10.1111/arcm.12040.
Huelga-Suarez, G., Moldovan, M., Suárez Fernández, M., De Blas Cortina, M.Á., Vanhaecke, F., García Alonso, J.I., 2012. Lead isotopic analysis of copper ores from the Sierra El Aramo (Asturias, spain). Archaeometry 54, 685–697. https://doi.org/10.1111/j.1475-4754.2011.00635.x.
Huston, D.L., Champion, D.C., Ware, B., Carr, G., Maas, R., Tessalina, S., 2019. Preliminary national-scale lead isotope maps of Australia. Geosci. Aust, Rec, p. 01.
Jézégou, Marie-Pierre, Klein, Sabine, Rico, Christian, Domergue, Claude, 2011. Les lingots de cuivre de l'épave romaine Plage de la Corniche 6 à Sète et le commerce du cuivre hispanique en Méditerranée occidentale. Rev. archéologique Narbonnaise 44 (1), 57–69. https://doi.org/10.3406/ran.2011.1819.
Julivert, N., Fontboté, J.M., Ribeiro, A., Conde, L., 1972. Mapa Tectónico de la Península Ibérica y Baleares. E 1:1.000.000.
Killick, D., Stephens, J., Fenn, T.R., 2020. Geological constraints on the use of lead isotopes for provenance in archaeometallurgy. Archaeometry arcm.12573. https://doi.org/10.1111/arcm.12573.
Lillo, Javier, 1992. Vein-type base-metal ores in Linares-La Carolina (Spain): ore-lead isotopic constrains. Eur. J. Mineral. 4 (2), 337–344. https://doi.org/10.1127/ejm/4/2/0337.
Ludwig, K.R., 1999. ISOPLOT/Ex—A Geochronological Toolkit for Microsoft Excel, Version 2.05. Geochronol. Cent. Spec. Publ. 1a.
Lunar, R., Moreno, T., Lombardero, M., Regueiro, M., López-Vera, F., Martínez del Olmo, W., Mallo García, J.M., de Santa, Saenz, Maria, J.A., García-Palomero, F., Higueras, P., Ortega, L., Capote, R., 2002. Economic and Environmental Geology. In: Gibbons, W., Moreno, T. (Eds.), The Geology of Spain. The Geological Society of London, London, pp. 473–510 https://doi.org/10.1144/GOSPP.19.
Marcoux, É., Pascual, E., Onézime, J., 2002. Hydrothermalisme anté-Hercynien en Sud-Ibérie : apport de la géochimie isotopique du plomb. Comptes Rendus Geosci. 334, 259–265. https://doi.org/10.1016/S1631-0713(02)01734-0.
Mederos Martín, A., Chamón Fernández, J., García Alonso, J.I., 2017. Análisis de isótopos de plomo de lingotes de estaño del pecio fenicio del Bajo de la Campana (Murcia, España), in: Martínez Alcalde, M., García Cano, J.M., Blánquez Pérez, J., Iniesta Sanmartín, A. (Eds.), Mazarrón II: Contexto, Viabilidad y Perspectivas Del Barco B-2 de La Bahía de Mazarrón : En Homenaje a Julio Mas García. pp. 429–443.
Molofsky, L.J., Killick, D., Ducea, M.N., Macovei, M., Chesley, J.T., Ruiz, J., Thibodeau, A., Popescu, G.C., 2014. A novel approach to lead isotope provenance studies of tin and bronze: Applications to South African, Botswanan and Romanian artifacts. J. Archaeol. Sci. 50, 440–450. https://doi.org/10.1016/j.jas.2014.08.006.
Montero Ruiz, I., 2018. La procedencia del metal: consolidación de los estudios con isótopos de plomo en la Península Ibérica, Revista d'arqueologia de Ponent. https://doi.org/10.21001/rap.2018.28.17.
Moorbath, S.E., 1962. Lead isotope abundance studies on mineral occurrences in the British Isles and their geological significance. Philos. Trans. R. Soc. London. Ser. A. Math. Phys. Sci. 254, 295–360. https://doi.org/10.1098/rsta.1962.0001.
Muñoz, J.A., 2019. Alpine Orogeny: Deformation and Structure in the Northern Iberian Margin (Pyrenees s.l.). pp. 433–451. https://doi.org/10.1007/978-3-030-11295-0_9.
Nier, Alfred O., 1938. Variations in the Relative Abundances of the Isotopes of Common Lead from Various Sources. J. Am. Chem. Soc. 60 (7), 1571–1576. https://doi.org/10.1021/ja01274a016.
Nocete, F., Sáez, R., Navarro, A.D.D., San Martin, C., Gil-Ibarguchi, J.I.I., 2018. The gold of the Carambolo Treasure: New data on its origin by elemental (LA-ICP-MS) and lead isotope (MC-ICP-MS) analysis. J. Archaeol. Sci. 92, 87–102. https://doi.org/10.1016/j.jas.2018.02.011.
Palero-Fernández, F.J., Martin-Izard, A., Prieto, M.Z., Mansilla-Plaza, L., Prieto, Z., Mansilla-Plaza, L., 2015. Geological context and plumbotectonic evolution of the giant Almadén mercury deposit. Ore Geol. Rev. 64, 71–88. https://doi.org/10.1016/j.oregeorev.2014.06.013.
Pernicka, E., 2014. Provenance Determination of Archaeological Metal Objects. In: Roberts, B.W., Thornton, C.P. (Eds.), Archaeometallurgy in Global Perspective. Springer, New York, New York, NY, pp. 239–268. https://doi.org/10.1007/978-1-4614-9017-3_11.
Pernicka, Ernst, 1995. Crisis or Catharsis in Lead Isotope Analysis? J. Mediterr. Archaeol. 8 (1), 59–64.
Pollard, A.M., 2018. Beyond Provenance New Approaches to Interpreting the Chemistry of Archaeological Copper Alloys, Studies in Archaeological Sciences. Leuven University Press, Leuven, Belgium.
Pollard, A.M., 2009. What a long, strange trip it's been. In: Shortland, A.J., Freestone, I. C., Rehren, T. (Eds.), From Mine to Microscope, Advances in the Study of Ancient Technology. Oxbow Books, pp. 181–190.
Quesada, C., Oliveira, J.T. (Eds.), 2019. The Geology of Iberia: A Geodynamic Approach, Regional Geology Reviews. Springer International Publishing, Cham. https://doi.org/10.1007/978-3-030-10519-8.
Quirt, David, Benedicto, Antonio, 2020. Lead Isotopes in Exploration for Basement-Hosted Structurally Controlled Unconformity-Related Uranium Deposits: Kiggavik Project (Nunavut, Canada). Minerals 10 (6), 512. https://doi.org/10.3390/min10060512.
Radivojević, Miljana, Roberts, Benjamin W., Pernicka, Ernst, Stos-Gale, Zofia, Martinón-Torres, Marcos, Rehren, Thilo, Bray, Peter, Brandherm, Dirk, Ling, Johan, Mei, Jianjun, Vandkilde, Helle, Kristiansen, Kristian, Shennan, Stephen J., Broodbank, Cyprian, 2019. The Provenance, Use, and Circulation of Metals in the European Bronze Age: The State of Debate. Journal of Archaeological Research. Springer, US. 27 (2), 131–185. https://doi.org/10.1007/s10814-018-9123-9.
Reguera-Galan, A., Barreiro-Grille, T., Moldovan, M., Lobo, L., Blas Cortina, M.Á., García Alonso, J.I., 2019. A Provenance Study of Early Bronze Age Artefacts Found in Asturias (Spain) by Means of Metal Impurities and Lead, Copper and Antimony Isotopic Compositions. Archaeometry 61 (3), 683–700. https://doi.org/10.1111/arcm.12445.
Rodríguez Vinceiro, F., Murillo Barroso, M., Fernández Rodriguez, L.-E., Montero Ruiz, I., 2018. Metalurgia prehistórica en Tierras de Antequera y su contexto andaluz. Zephyrvs 81, 93. https://doi.org/10.14201/zephyrus20188193115.
Rubio-Ordóñez, A., Gutiérrez-Alonso, G., Valverde-Vaquero, P., Cuesta, A., Gallastegui, G., Gerdes, A., Cárdenes, V., 2015. Arc-related Ediacaran magmatism along the northern margin of Gondwana: Geochronology and isotopic geochemistry from northern Iberia. Gondwana Res. 27 (1), 216–227. https://doi.org/10.1016/j.gr.2013.09.016.

Russell, R.D., Farquhar, R.M., 1961. Lead Isotopes in Geology. Geol. Mag. 98, 174–174.
Schibille, N., De Juan Ares, J., Casal García, M.T., Guerrot, C., 2020. Ex novo development of lead glassmaking in early Umayyad Spain. Proc. Natl. Acad. Sci. U. S. A. https://doi.org/10.1073/pnas.2003440117.
Simancas, J.F., Abad, I., Almodovar, G.R., Castro, A., de la Rosa, J.D., Donaire, T., González, F., Moreno, C., Nieto, F., Pascual, E., Saez, R., Sierra, S., Valenzuela, A., Velilla, N.S., 2004. Zona Sudportuguesa. In: Vera, J.A. (Ed.), Geología de España. SGE-IGME, Madrid, pp. 199–222.
Sinner, A.G., Ferrante, M., Nisi, S., Trincherini, P.R., 2020. Lead isotope evidence of lead supply in ancient Ilduro (second-first centuries B.C.E.). Archaeol. Anthropol. Sci. 12, 131. https://doi.org/10.1007/s12520-020-01073-7.
Stacey, J.S., Kramers, J.D., 1975. Approximation of terrestrial lead isotope evolution by a two-stage model. Earth Planet. Sci. Lett. 26 (2), 207–221. https://doi.org/10.1016/0012-821X(75)90088-6.
Stannard, C., Sinner, A.G., Ferrante, M., 2019. Trade between Minturnae and Hispania in the Late Republic. Numis. Chron. 179, 123–171. https://doi.org/10.17613/xv02-v750.
Stos-Gale, Z., 2001. The impact of the natural sciences on studies of Hacksilber and early silver coinage. In: Balmuth, M. (Ed.), Hacksilber to Coinage: New Insights into the Monetary History of the Near East and Greece. Numismatic Studies 24. The American Numismatic Society, New York, pp. 53–76.
Stos-Gale, Zofia Anna, Gale, Noël H., 2009. Metal provenancing using isotopes and the Oxford archaeological lead isotope database (OXALID). Archaeol. Anthropol. Sci. 1 (3), 195–213. https://doi.org/10.1007/s12520-009-0011-6.
Stos-Gale, Z.A., Hunt-Ortiz, M.A., Gale, N.H., 1999. Análisis elemental y de isótopos de plomo de objetos metálicos de Gatas, in: Proyecto Gatas. 2 : Ia Dinamica Arqueoecológica de Ia Ocupación Prehistórica.
Subías, I., Fanlo, I., Billström, K., 2015. Ore-forming timing of polymetallic-fluorite low temperature veins from Central Pyrenees: A Pb, Nd and Sr isotope perspective. Ore Geol. Rev. 70, 241–251. https://doi.org/10.1016/j.oregeorev.2015.04.013.
Thompson, C., Skaggs, S., 2013. King Solomon's Silver? Southern Phoenician Hacksilber Hoards and the Location of Tarshish. Internet Archaeol. https://doi.org/10.11141/ia.35.6.
Tornos, F., Chiaradia, M., 2004. Plumbotectonic Evolution of the Ossa Morena Zone, Iberian Peninsula: Tracing the Influence of Mantle-Crust Interaction in Ore-Forming Processes. Econ. Geol. 99 (5), 965–985. https://doi.org/10.2113/gsecongeo.99.5.965.
Velasco, F., Pesquera, A., Herrero, J.M., 1996. Lead isotope study of Zn-Pb ore deposits associated with the Basque-Cantabrian basin and Paleozoic basement, Northern Spain. Miner. Depos. 31, 84–92. https://doi.org/10.1007/BF00225398.
Vera, J.A. (Ed.), 2004. Geología de España. Sociedad Geológica de España, IGME.
Villa, I.M., 2016. Provenancing Bronze: Exclusion, Inclusion, Uniqueness, and Occam's Razor. In: Grupe, G., McGlynn, G.C. (Eds.), Isotopic Landscapes in Bioarchaeology. Springer Berlin Heidelberg, Berlin, Heidelberg, pp. 141–154. https://doi.org/10.1007/978-3-662-48339-8_8.
Wagner, R., 2000. Searching ancient copper sources – a lead isotope study of Roman bronze vessels from Pompeii. Kölner Jahrb. 33, 615–616.
Westner, K.J., Birch, T., Kemmers, F., Klein, S., Höfer, H.E., Seitz, H.-M., 2020. ROME'S Rise to Power. Geochemical Analysis of Silver Coinage from the Western Mediterranean (Fourth to Second Centuries BCE). Archaeometry 62 (3), 577–592. https://doi.org/10.1111/arcm.12547.
Wood, Jonathan R., Montero-Ruiz, Ignacio, 2019. Plata semirrefinada para los plateros de la Edad del Hierro en el Mediterráneo: un mecanismo para identificar la plata ibérica. Trab. Prehist. 76 (2), 272. https://doi.org/10.3989/tp.2019.12237.
Zhu, Bingquan, 1995. The mapping of geochemical provinces in China based on Pb isotopes. J. Geochemical Explor. 55 (1-3), 171–181. https://doi.org/10.1016/0375-6742(95)00011-9.